Neutrino Detection at the 100 MeV Scale and Beyond

Brooke Russell (MIT)

17th International Neutrino Summer School @ UC Santa Barbara

June 29, 2026

The Russell Group

Neutrino physics @ DUNE
Low-mass particle dark matter searches
Weak interaction phenomenology

Brooke Russell
Assistant Professor

A.B. Princeton ’11
Ph.D. Yale ‘20
Chamberlain Fellow @ LBNL ‘20-’23
Pappalardo Fellow @ MIT ‘24-’25

Cecilia Ferrari
Postdoc

Thomas Barbera
Graduate student

Corey Romanov
Postbac

Lars Bathe-Peters
Incoming postdoc

Christopher Prainito
Incoming graduate student

2x2Demonstrator in NuMI

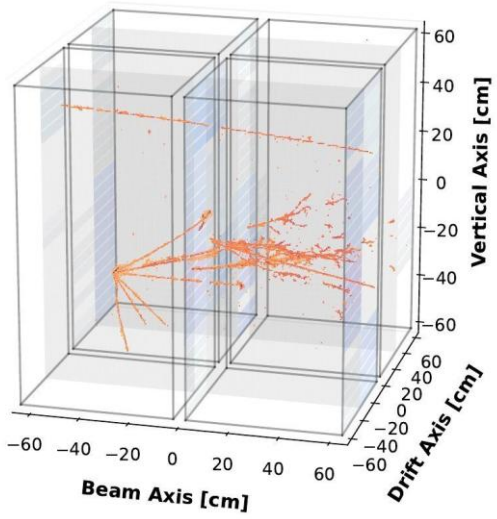

Low-mass DM absorption with amorphous solids

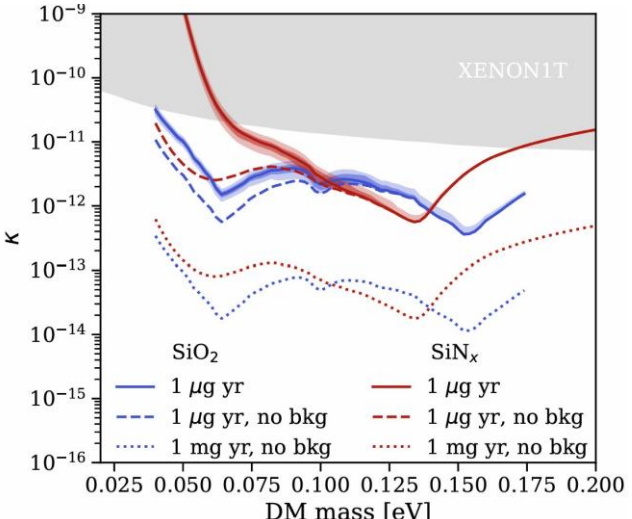

First experimental bound on the thermal solar neutrino flux

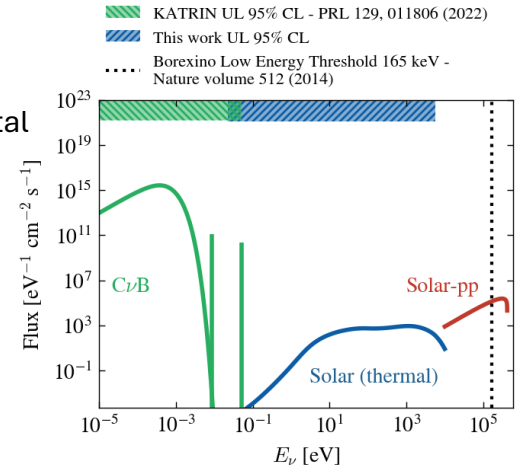

The Plan

Lecture 1 (today)

- Motivate neutrino detection inference through *detector response*
  - ➔ Establish the framework for important aspects of detector design

Lecture 2 (tomorrow)

- Neutrino flux specific *full response* (detector response ⊗ electronics response) optimization
  - ➔Modern accelerator-based neutrino experiment case studies in instrument application

Content shown here is germane to >100 MeV neutrino detection

➔ See P. Barbeau for <100 MeV neutrino detection

Resources

Papers

F. Takahashi *et al.* (Particle Data Group), to be published in Int. J. Mod. Phys. A **41**, 2630011 (2026)

P. Barbeau, P. Merkel, J. Zhang, “Instrumentation Frontier”, Snowmass 2021 IF Report.

ECFA Detector R&D Roadmap Process Group, “The 2021 ECFA Detector Research and Development Roadmap”, CERN-ESU-017 (2021)

Books

W.R. Leo, *Techniques for Nuclear and Particle Physics Experiments: A How-to Approach,* 2nd ed., Springer-Verlag, 1994.

R.C. Fernow, *Introduction to Experimental Particle Physics*, Cambridge University Press, 1986

G.F. Knoll, *Radiation Detection and Measurement*, 4th ed., Wiley, 2010.

Slides

J. Raaf, “Neutrino Detectors”, INSS, Fermilab 2025.

M. Messier, “Neutrino Detectors”, Neutrino University, Fermilab 2025.

M. Mager, “Detector Technologies”, CERN-Fermilab HCP Summer School, CERN 2025.

By the end of this talk, you should understand the following:

- ❑ How to “flavor tag” neutrino interactions
- ❑ Why charged leptons have specific detection characteristics
- ❑ How neutral current interactions can “fake” charged current interactions
- ❑ How to account for final state neutrons, to some degree

Outline

I. Neutrino detection
II. Signal creation
III. Principles of instrument detection & measurement

➔ See P.B. Denton for discussion on neutrino properties

Neutrino detection

Force	Relative Intensity
Strong	~1
Electromagnetic	~10^{-3}
Weak	~10^{-5}
Gravity	~10^{-38}

Neutrinos interact solely through the weak force which is extremely short range
We **infer** neutrino interactions from *observable* final state particle kinematics

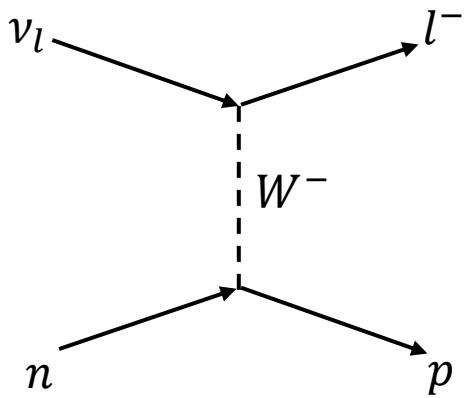

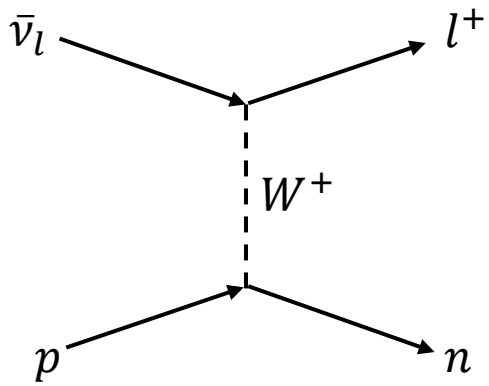

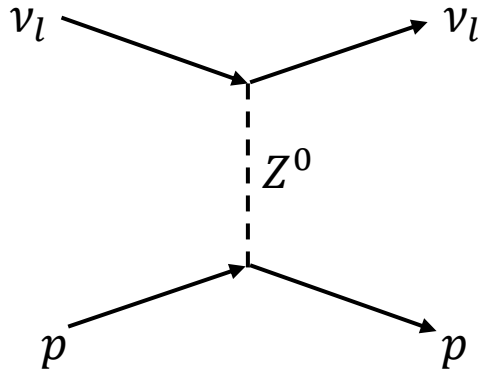

In charged current interactions, the *outgoing charged lepton* identifies *the incoming neutrino flavor*

N.B. charged lepton production threshold must be taken into account
E.g. $E_{\nu_\tau} \gtrsim 3.35$ GeV for $\nu_\tau + N \rightarrow \tau + N$

*The above are nonexhaustive examples of neutrino interactions for illustration purposes

Outline

I. Neutrino detection
II. Signal creation
III. Principles of instrument detection & measurement

Passage of Radiation through Matter

Incident Radiation Features:

- Energy loss
  - Collision
  - Radiation
- Trajectory deflection
  - Inelastic atomic collisions
  - Elastic scattering with nuclei

Passage of Radiation through Matter

Incident Radiation Features:

- Energy loss
  - Collision
  - Radiation
- Trajectory deflection
  - Inelastic atomic collisions
  - Elastic scattering with nuclei

Target Medium Effects:

- Detector response
  - Ionization
  - Atomic/nuclear excitation
    - Photon
    - Phonon
    - Roton
- Characteristic tracking topologies
  - Blips
  - Tracks
  - Showers

Passage of Radiation through Matter

Incident Radiation Features:

- Energy loss
  - Collision
  - Radiation
- Trajectory deflection
  - Inelastic atomic collisions
  - Elastic scattering with nuclei

Interaction particle class dependency:

- “heavy” charged particles*
- Electrons and positrons
- Photons
- Neutrons

Target Medium Effects:

- Detector response
  - Ionization
  - Atomic/nuclear excitation
    - Photon
    - Phonon
    - Roton
- Characteristic tracking topologies
  - Blips
  - Tracks
  - Showers

Detector measurements

*Applicable to particles heavier than an electron and lighter than heavy ions

“Heavy” Charged Particle Energy Loss

Bethe-Bloch formula: material dependent particle mean energy loss $\left\langle \frac{dE}{dx} \right\rangle$ parameterization as a function of momentum transfer $\beta\gamma$

➔ Builds on Bohr’s classical electronic collision loss by charged particles parameterized by impact parameter, taking into account quantum effects

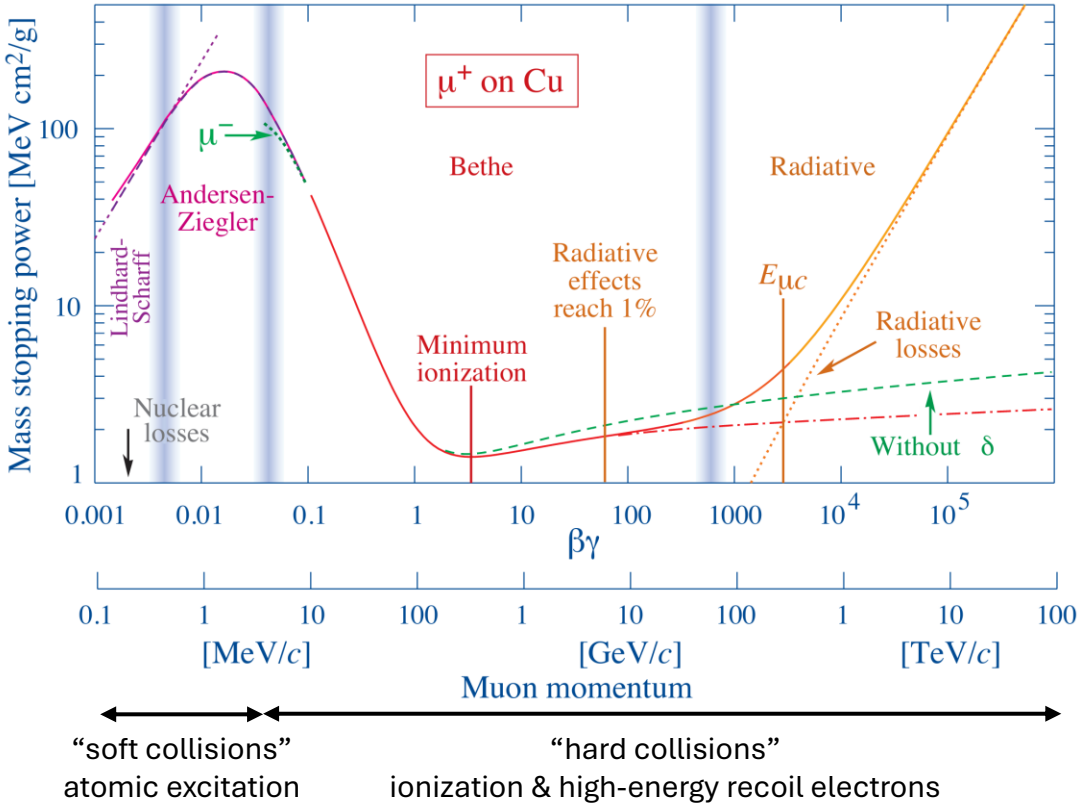

$$\left\langle -\frac{dE}{dx} \right\rangle = Kz^2 \frac{Z}{A} \frac{1}{\beta^2} \left[\frac{1}{2} ln \frac{2m_e c^2 \beta^2 \gamma^2 W_{max}}{I^2} - \beta^2 - \frac{\delta(\beta\gamma)}{2} - \frac{C(\beta)}{Z} + zL_1(\beta) + z^2 L_2(\beta) \right]$$

“Heavy” Charged Particle Energy Loss

Bethe-Bloch formula:

K: coefficient in units of MeV mol^{-1} cm^2
z: charge number of incident particle
A: atomic mass of absorber
Z: atomic number of absorber
m_e: electron mass
W_{max}: max energy transfer to an electron in a single collision
I: mean excitation energy

incident radiation dependence
target material dependence

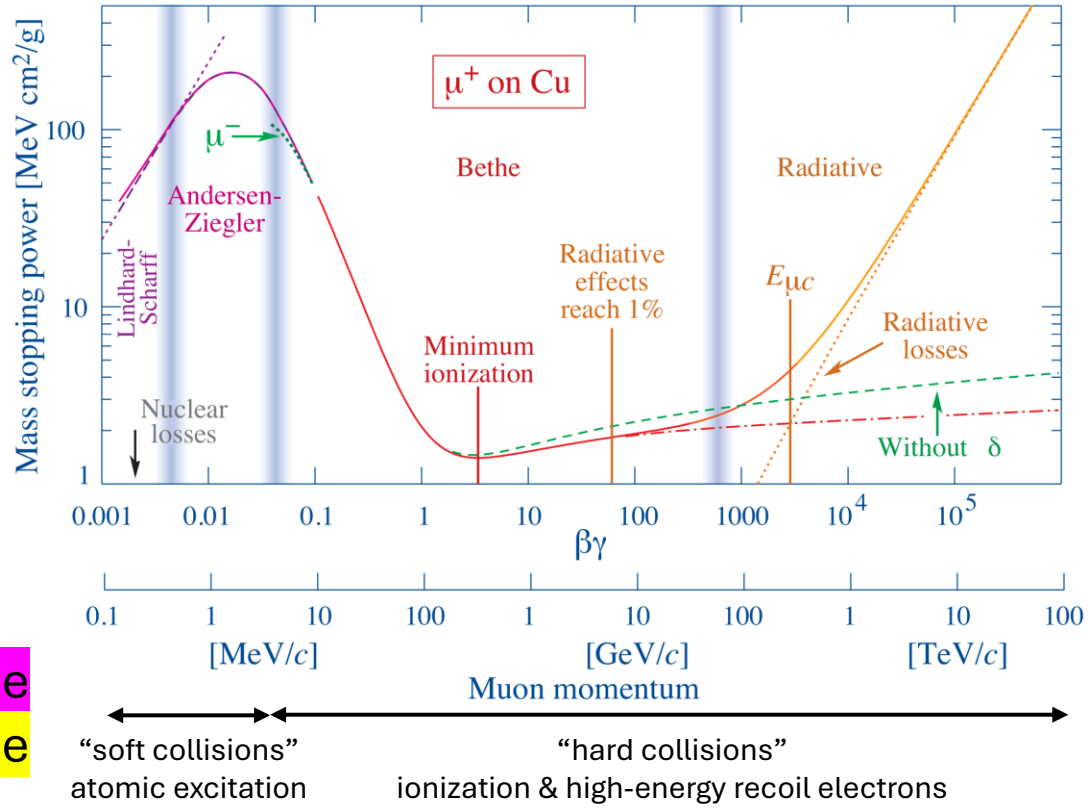

$$\left\langle -\frac{dE}{dx} \right\rangle = Kz^2 \frac{Z}{A} \frac{1}{\beta^2} \left[\frac{1}{2} ln \frac{2m_e c^2 \beta^2 \gamma^2 W_{max}}{I^2} - \beta^2 - \frac{\delta(\beta\gamma)}{2} - \frac{C(\beta)}{Z} + zL_1(\beta) + z^2 L_2(\beta) \right]$$

Bethe-Bloch High-Energy Corrections: Density Effect

Consequence of particle electric field polarizing atoms along its path

- Electrons far from the path of the particle are shielded from the full $\vec{E}$ intensity
  - Induced polarization greater in dense materials
- Outer-lying electrons contribute less to energy loss
  - As particle velocity increases outer-lying electrons contribute more

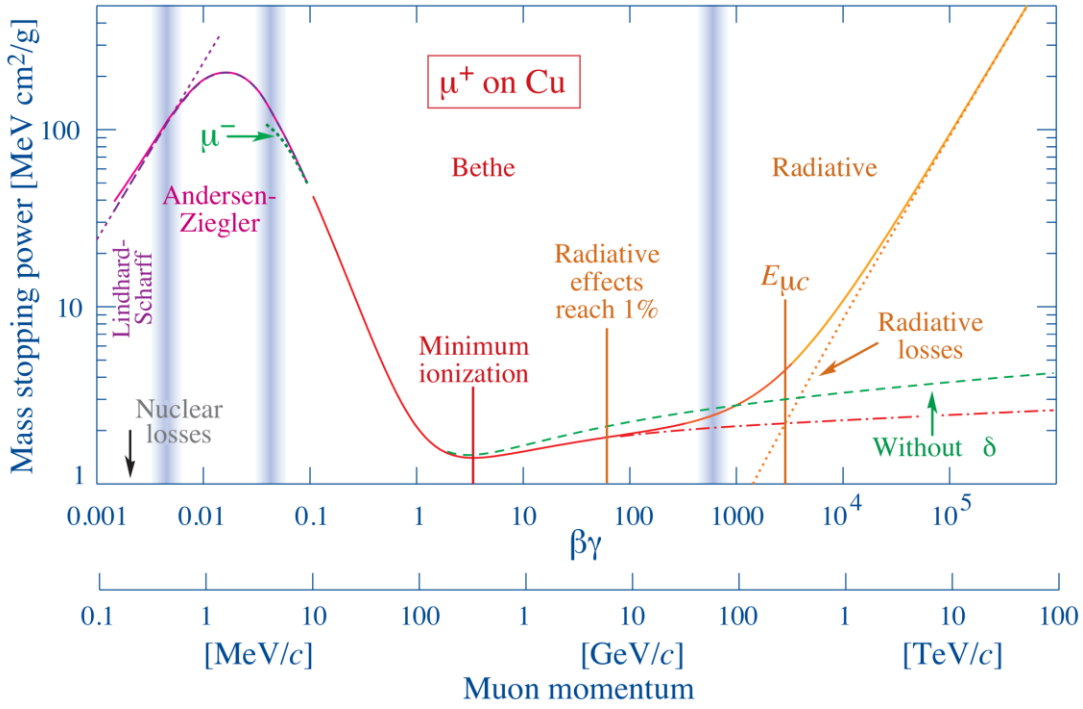

$$\left\langle -\frac{dE}{dx} \right\rangle = Kz^2 \frac{Z}{A} \frac{1}{\beta^2} \left[\frac{1}{2} ln \frac{2m_e c^2 \beta^2 \gamma^2 W_{max}}{I^2} - \beta^2 - \frac{\delta(\beta\gamma)}{2} - \frac{C(\beta)}{Z} + zL_1(\beta) + z^2 L_2(\beta) \right]$$

Bethe-Bloch Low-Energy Corrections

Accounts for effects when stationary electron assumption breaks down ➔ relevant when the incident particle velocity is comparable or smaller than the orbital velocity of atomic bound electrons

Shell correction: dE/dx contribution from K-, L-, M-shell electrons as particle velocity decreases
Barkas correction: electron cloud repulsion (attraction) for negatively (positively) charged particle
Bloch correction: accounts for perturbations of the atomic wave function

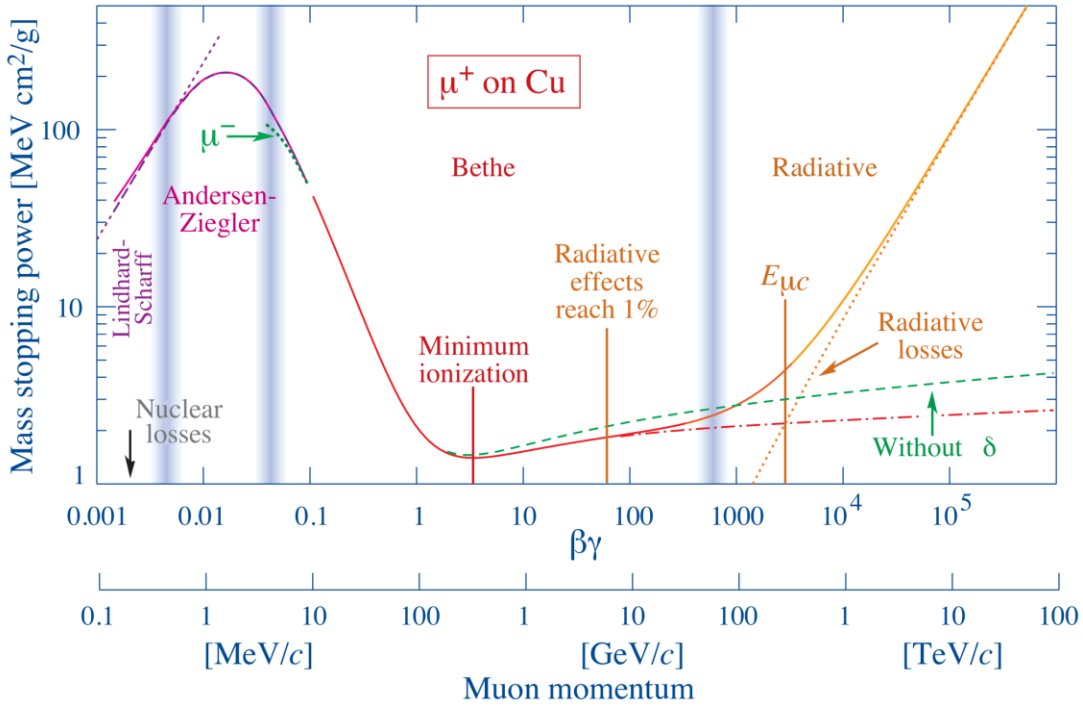

$$\left\langle -\frac{dE}{dx} \right\rangle = Kz^2 \frac{Z}{A}\frac{1}{\beta^2}\left[\frac{1}{2} ln \frac{2m_e c^2 \beta^2 \gamma^2 W_{max}}{I^2} - \beta^2 - \frac{\delta(\beta\gamma)}{2} - \boxed{\frac{C(\beta)}{Z}} + \boxed{zL_1(\beta)} + \boxed{z^2 L_2(\beta)}\right]$$

Bethe-Bloch $\beta\gamma$ Dependence

- MIP ionization energy loss for all materials (except hydrogen) in the 1-2 MeV/(g/cm^2)
- Marginal difference in $\left\langle \frac{dE}{dx} \right\rangle$ response for $\mu^{\pm}$ and $\pi^{\pm}$

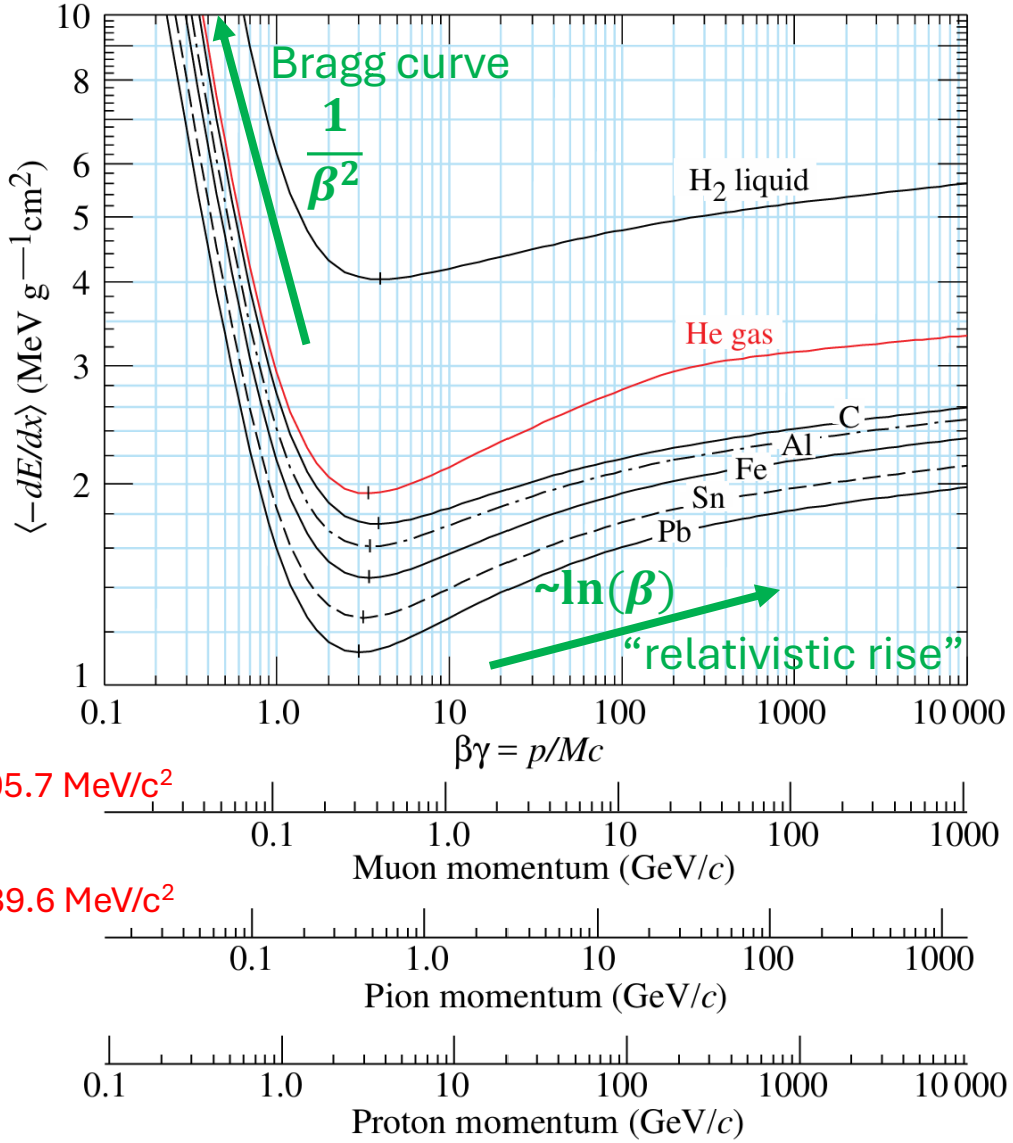

$m_{\mu^{\pm}}$ =105.7 MeV/c^2

$m_{\pi^{\pm}}$ =139.6 MeV/c^2

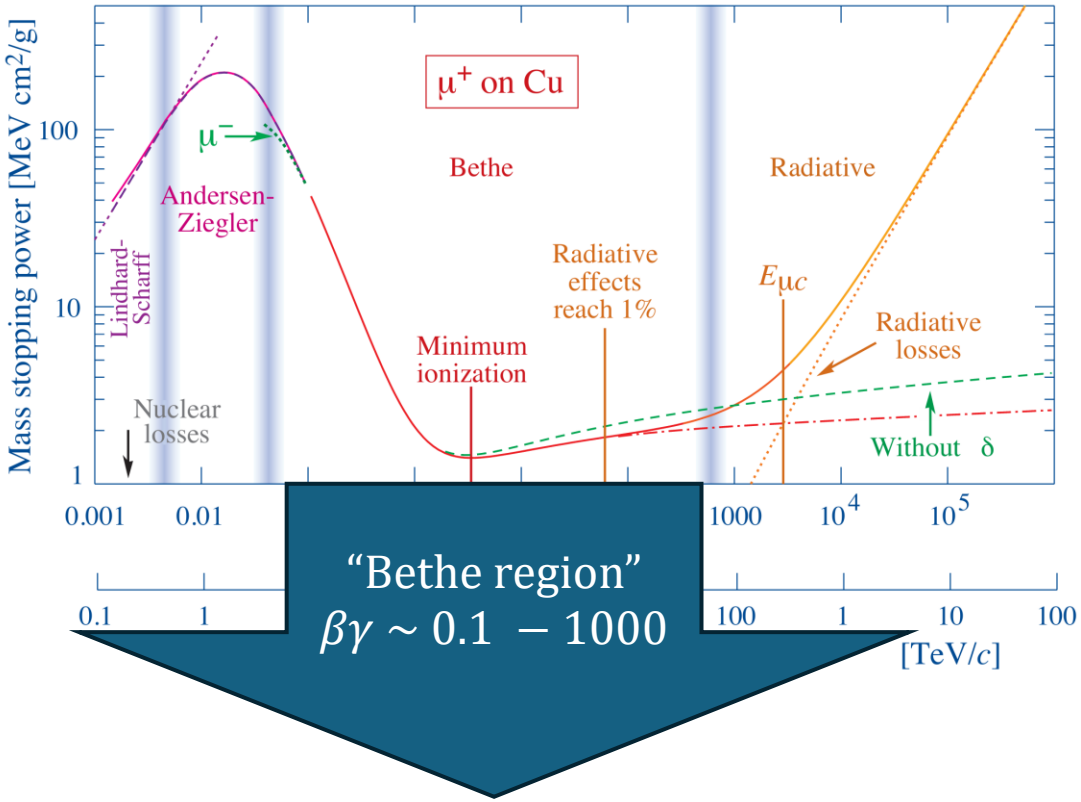

~100% ionization losses

Most heavy particles in accelerator-based neutrino experiments are in this range

Range

Assuming continuous energy loss, all identical particles with the same initial energy in the same type of material will traverse a defined distance

➢ See NIST stopping power and range tables*

Range straggling: an ensemble of identical particles will show a statistical distribution of ranges centered about the same mean value

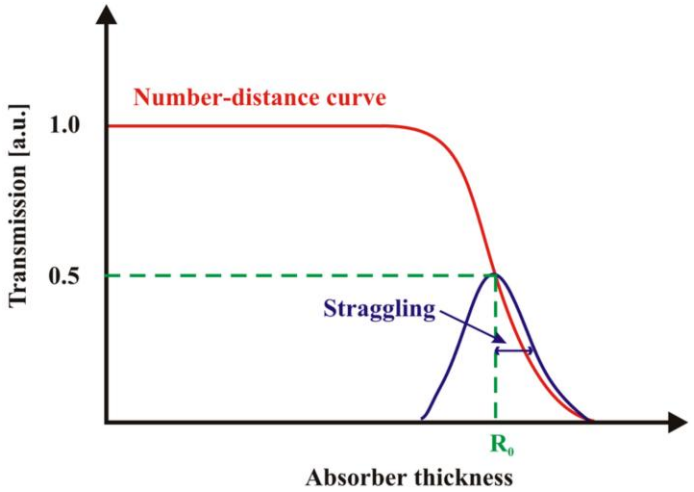

➢ Measure momentum by range of stopped particles

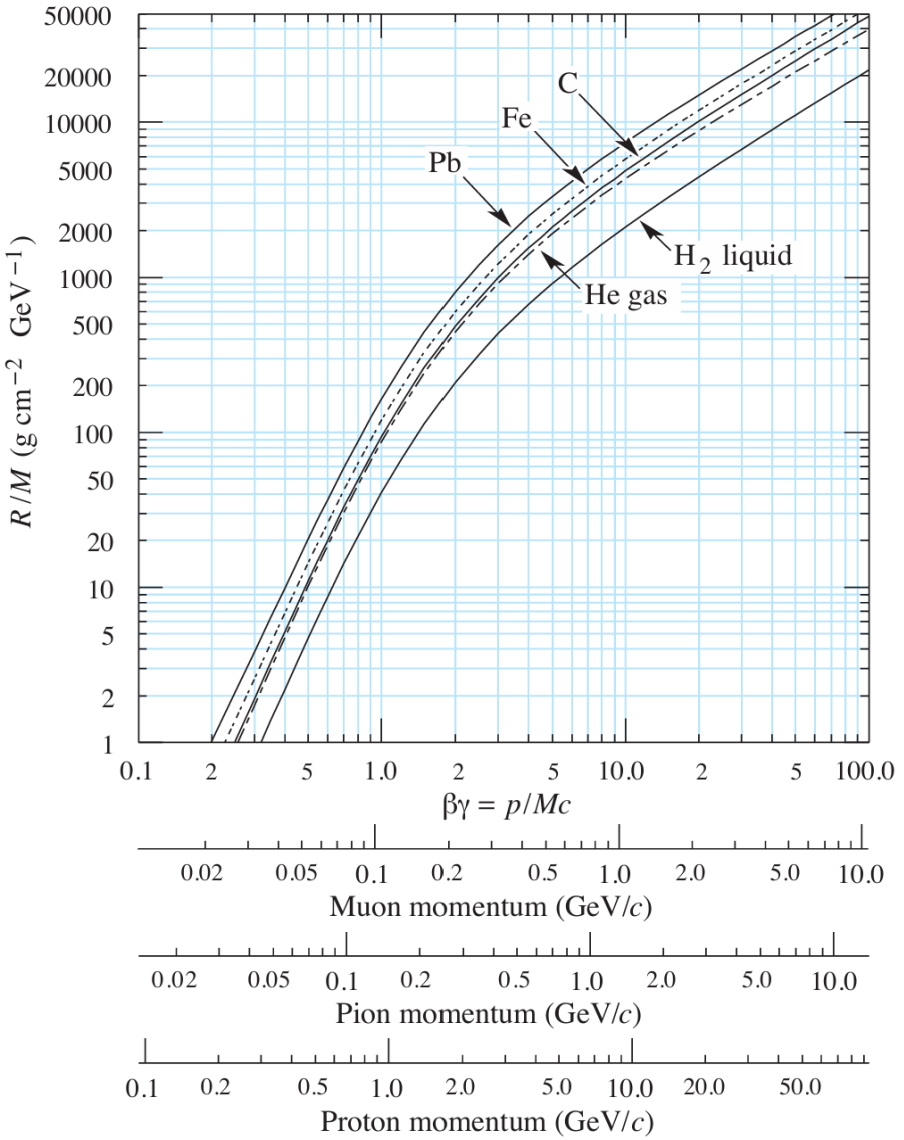

*Provided for electrons, protons, and helium ions

Particle Identification (PID) with dE/dx

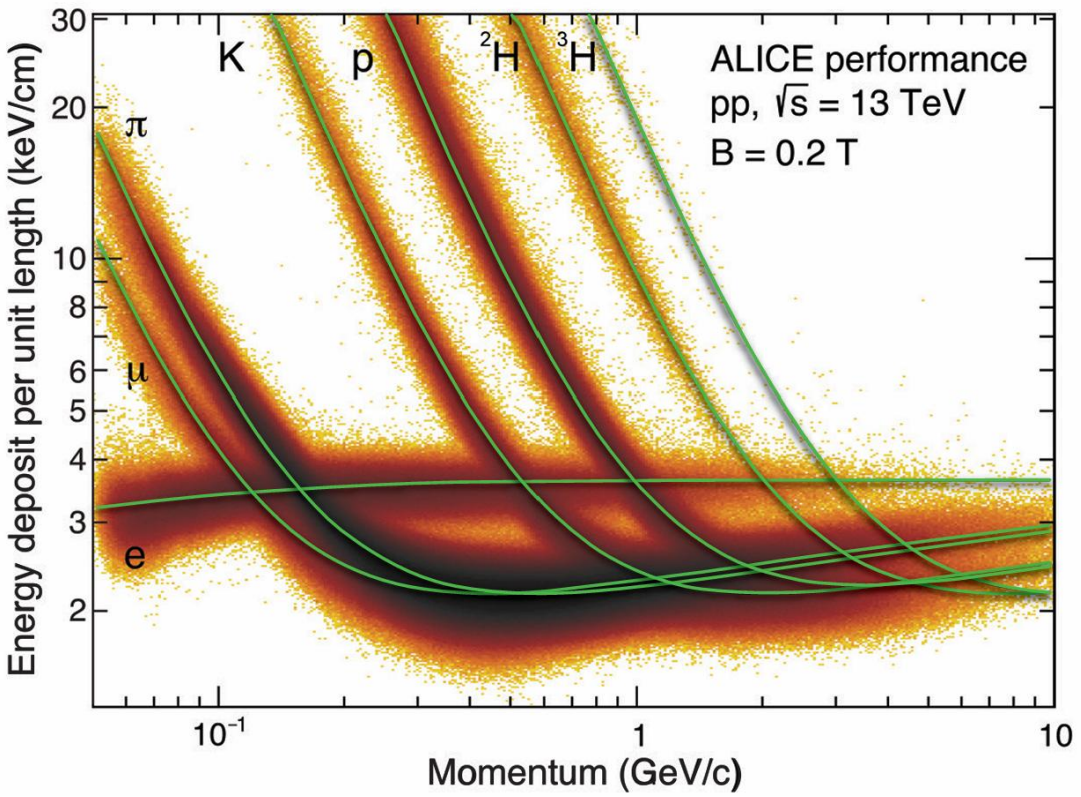

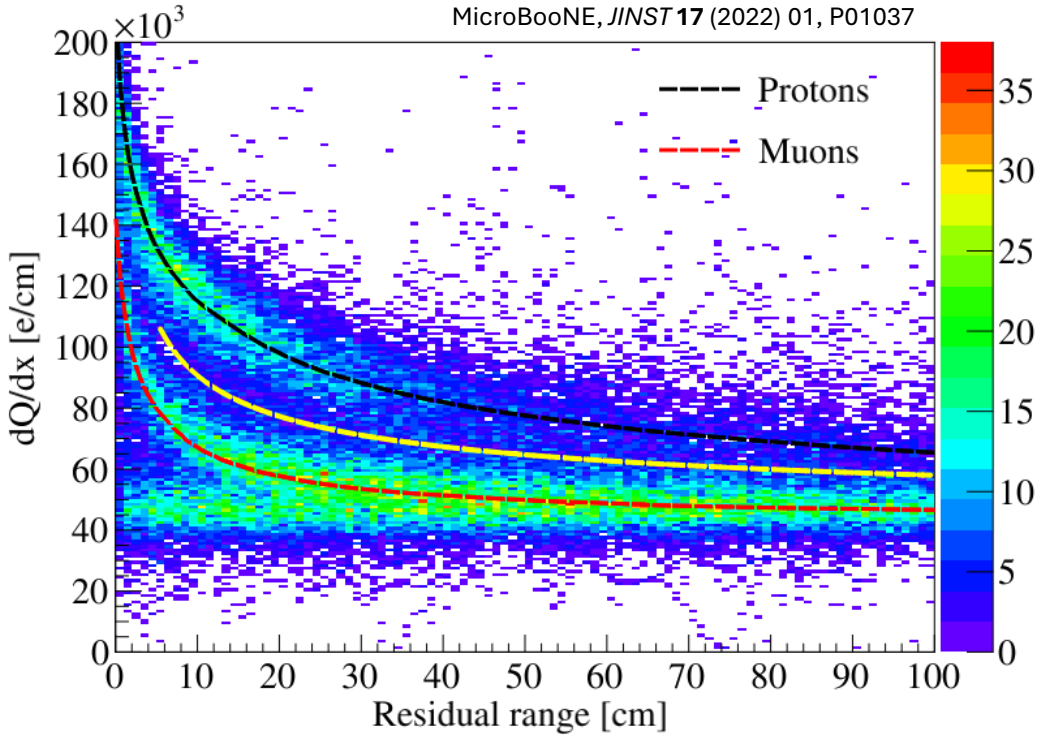

For a given momentum, $\frac{dE}{dx}$ is different for particles with different masses ➔ $\frac{dE}{dx} \propto \frac{m^2}{p^2}$

Energy Straggling

Fluctuations in the thickness of pathlength for a fixed loss in energy

$$\kappa = \frac{\overline{\Delta}}{W_{max}}$$

$\overline{\Delta}$ ≡mean energy loss

W_{max} ≡maximum energy transfer in a single collision

$\kappa \to 0$: Landau regime (thin absorbers more susceptible to single collision large energy transfer skewing the energy loss distribution)

κ~intermediate: Vavilov regime

$\kappa \to 1$: Gaussian regime (thick absorbers where the number of collisions is large)

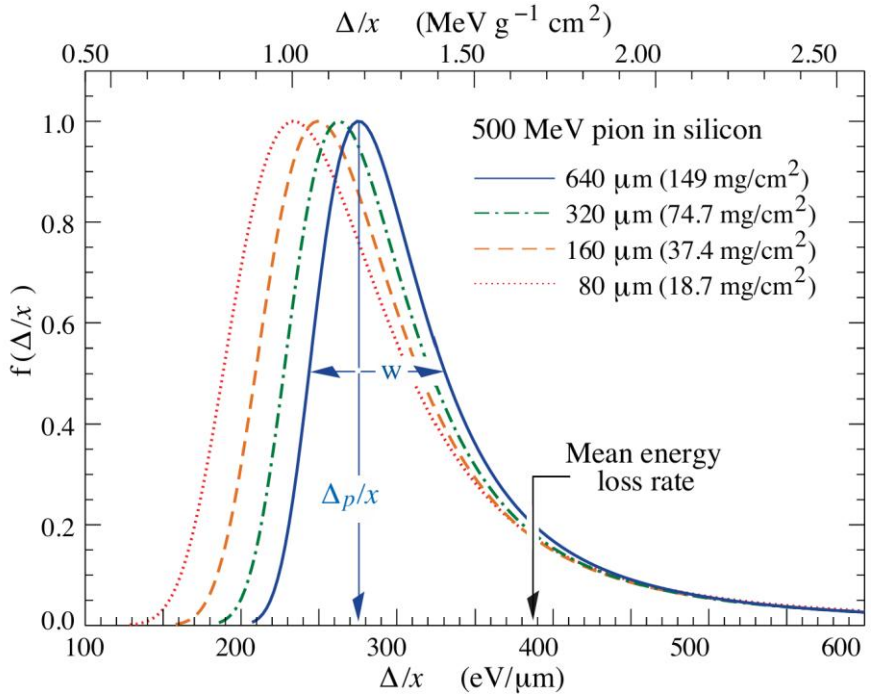

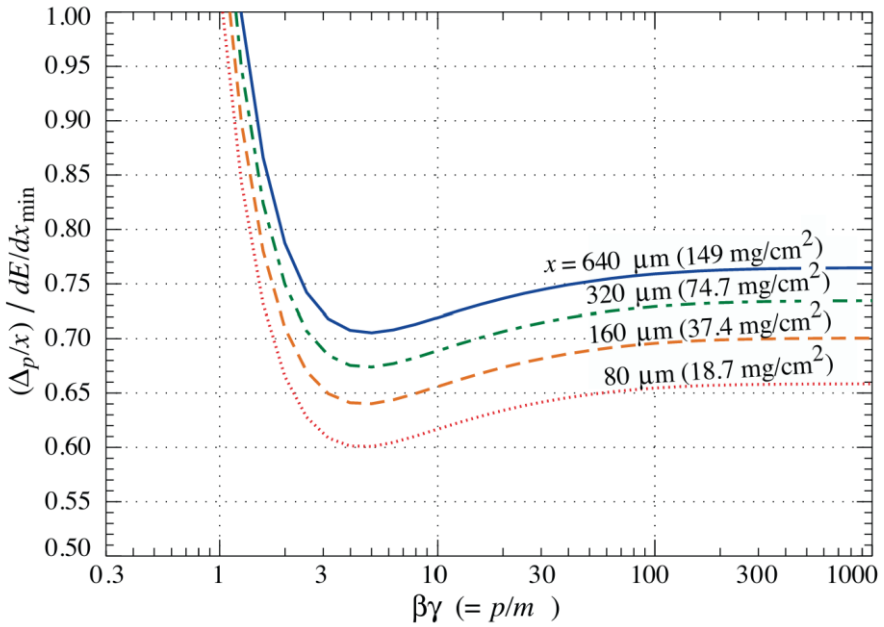

Multiple Coulomb Scattering

A charged particle traversing a material is deflected by many small-angle scatters in the electric fields of nuclei (Coulomb scattering)

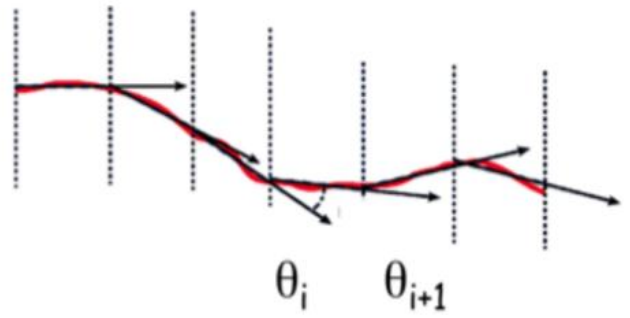

Statistical treatment on net angle of deflection of nuclear scatters as a function of thickness of material traversed can *resolve particle momentum for non-stopping tracks*

$$\theta_{MCS} = \frac{13.6\ MeV/c}{\beta p_i}\sqrt{\frac{L_{seg}}{X_0 cos\delta}}\frac{w_0}{cos\delta}$$

Applicable when the average number of independent scatters $N \geq 20$ and energy loss is small or negligible

- Straight track assumption fairly reliable for heavy particles of sufficient energy
- Electron trajectories are significantly by Coulomb scattering due to their light mass

Momentum by Curvature

Gargamelle, CERN-EX-1055

A particle with momentum p traveling through a uniform transverse magnetic field B will travel on a circle of radius ρ

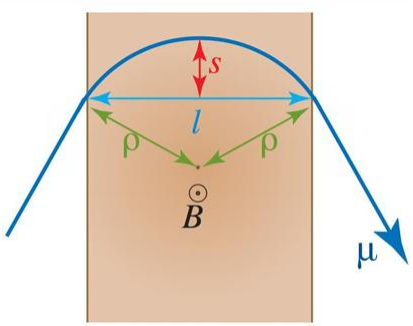

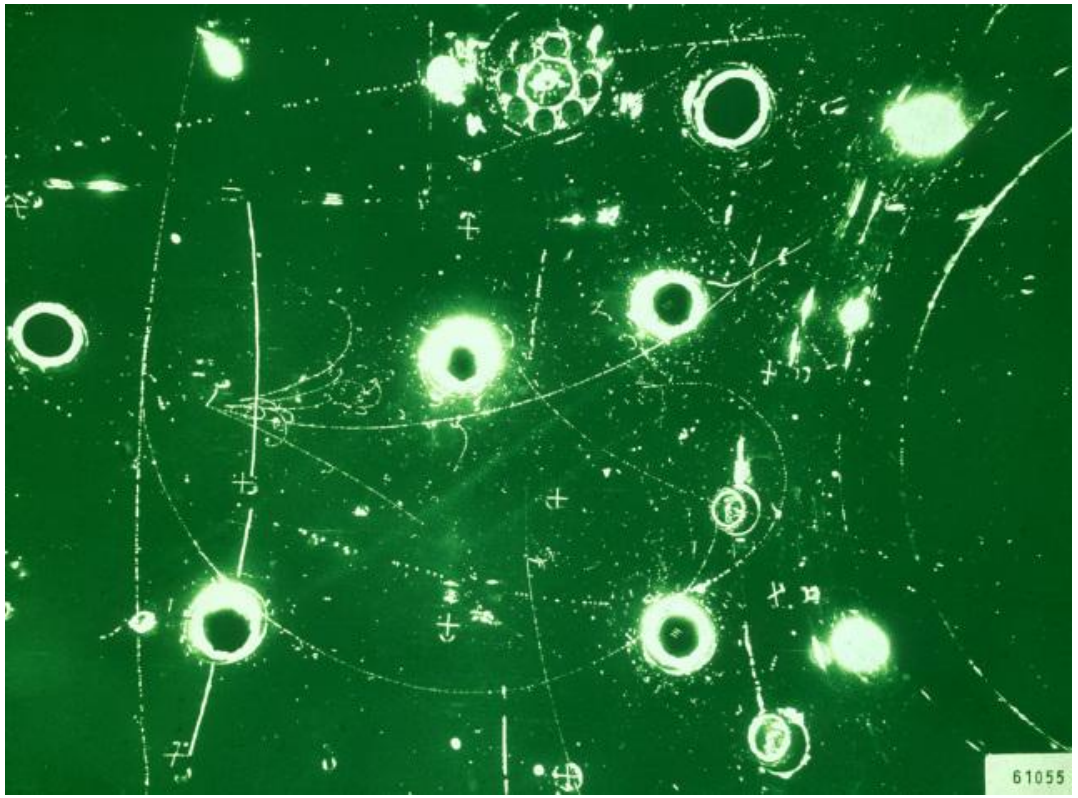

Measure the sagitta and chord of a track to determine its momentum:

$$p \simeq 0.3 \frac{bl^2}{8s}$$

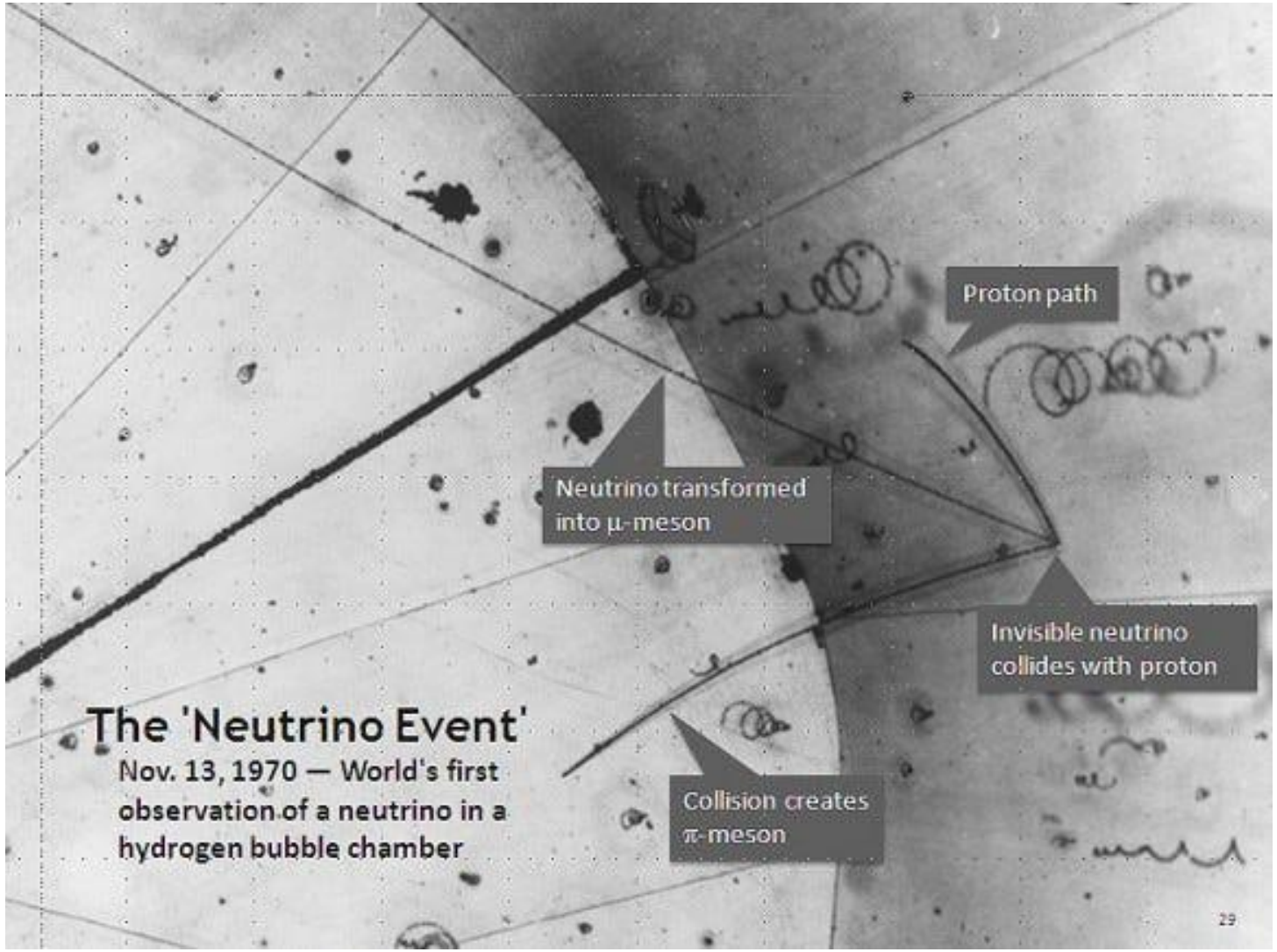
Proton path
Neutrino transformed into μ-meson
Invisible neutrino collides with proton
Collision creates π-meson
The 'Neutrino Event'
Nov. 13, 1970 — World's first observation of a neutrino in a hydrogen bubble chamber
29

Bethe-Bloch $\beta\gamma$ Dependence

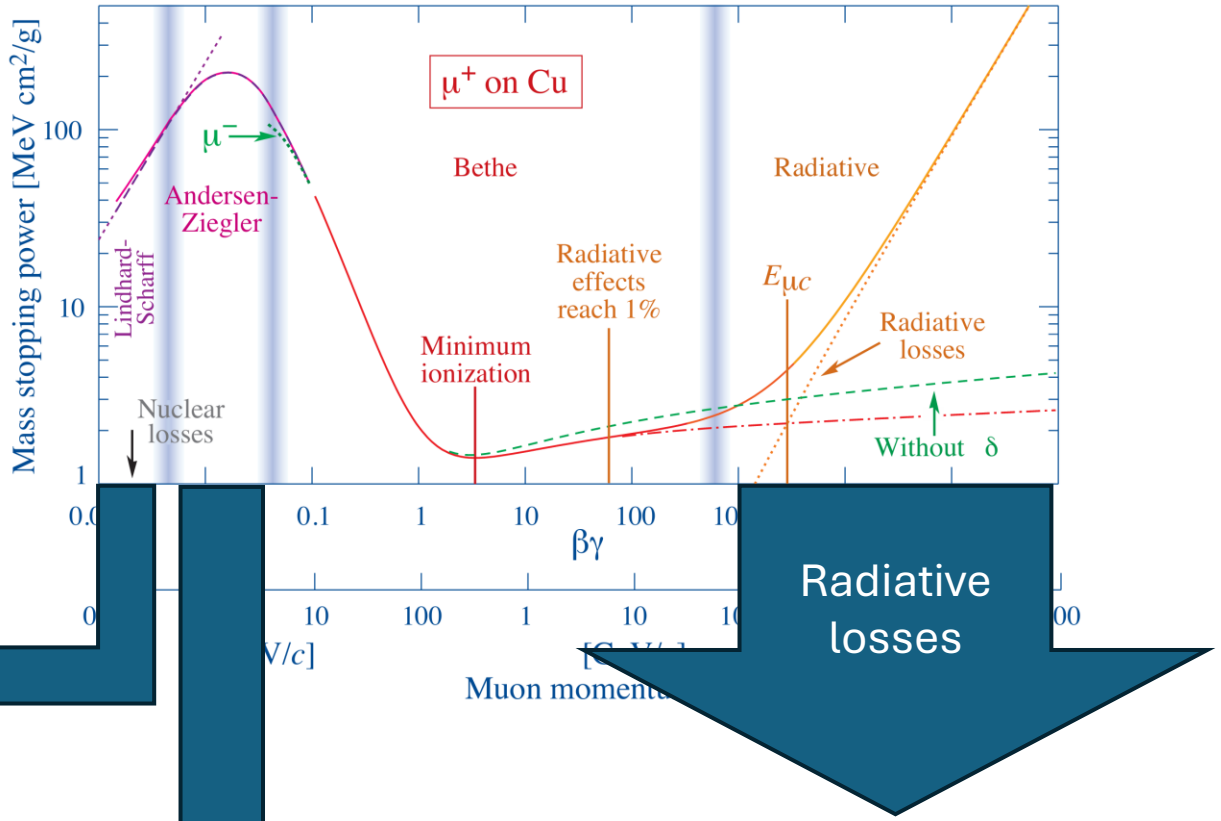

Energy loss reliably explained by Lindhard formulism

Bethe-Bloch breaks down ➔ assumptions invalid even with corrections

bremsstrahlung and delta ray production

Bremsstrahlung Radiation

Electromagnetic radiation emission from a charged particle scattering in the electric field of the nucleus producing *shower cascades*

- Dominant energy loss mechanism for heavy particles above $\beta\gamma \sim 1000$
- Due to their small mass, dominant energy loss mechanism at lower energies (~10-100 MeV) for electrons/positrons

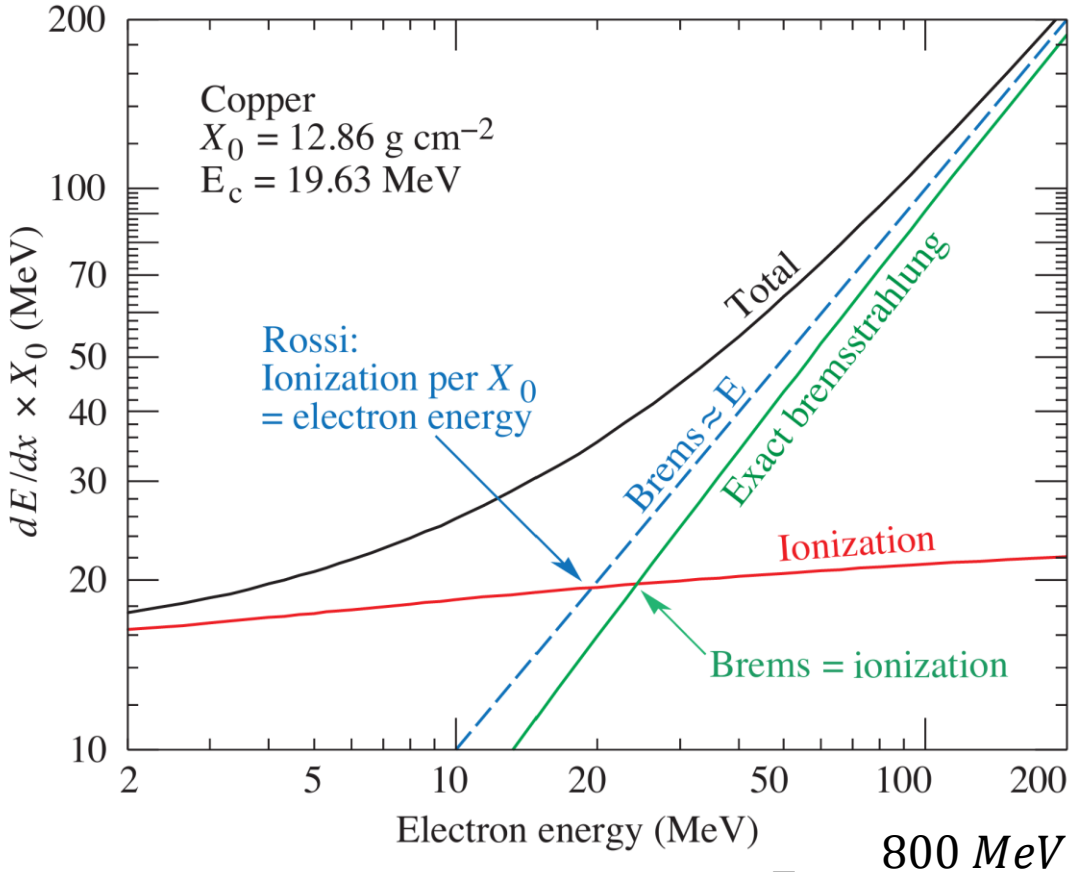

$$E_C = \frac{800\ MeV}{Z + 1.2}$$

Critical energy: bremsstrahlung energy loss is equivalent to energy loss by collision ionization

Hadronic Showers

Longitudinal development scales with nuclear absorption (interaction) length

$$\lambda = \frac{A}{N_A \sigma_{abs}}$$

After a strong interaction, ~half incident energy is passed to fast secondaries and the remainder is consumed in multiparticle production of slow pions

Cascade continues until secondary hadrons lose all their energy through collisions

Electromagnetic showers produced among hadronic shower cascade:

- hadron ionization range < λ ➔ track
- hadron ionization range > λ ➔ shower

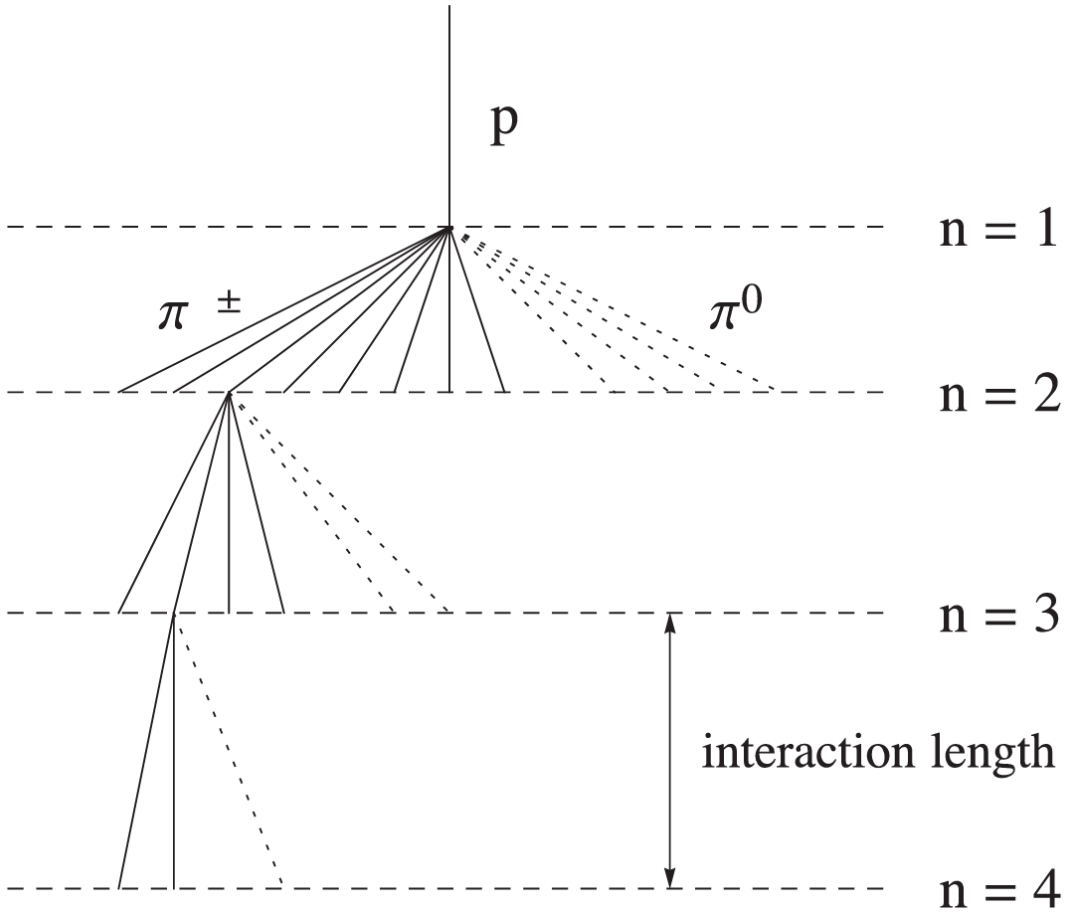

 J.M.C. Montanus, *Astropart. Phys.* 59 (2014) 4-11

Electromagnetic Showers

Shower development:

- e^+/e^- with $E > E_C$ travel one X_0, then bremsstrahlung a γ with *E/2*
- γ with $E > E_C$ travel $\lambda_{pair} = \frac{9}{7}X_0$, then pair produce e^+/e^- each with energy *E/2*
- Shower cascade continues until all electrons fall below the critical energy
  - Collisional energy loss for electrons
  - Compton scattering and photoelectric effect for photons

Relative to hadron showers:

- Exclusively EM showers
- Shallower and narrower for the same energy
- Better energy resolution

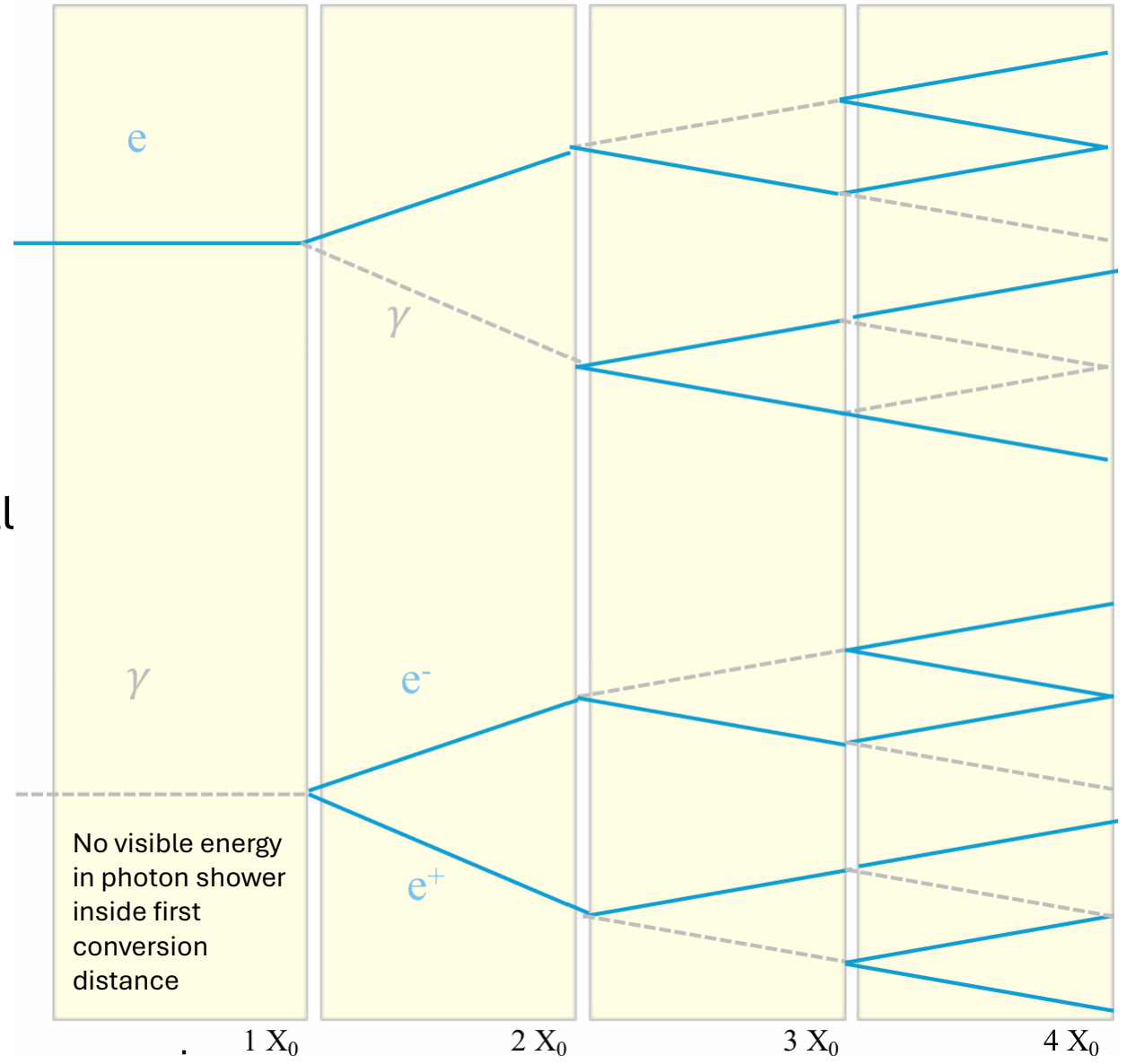

Radiation length (X_0): material dependent distance over which the electron energy is reduced by a factor of $\frac{1}{e}$ from bremsstrahlung

$$X_0 \simeq 180 \frac{A}{Z^2} \text{ g/cm}^2$$

Electromagnetic Shower Profiles

After t radiation lengths, the total number of particle will be $N \simeq 2^t$ with an average energy of $E(t) \simeq \frac{E_0}{2^t}$

Longitudinal shower maximum occurs at $t_{max} = ln\frac{E_0}{E_c} + C_i$ where

$C_i = -0.5$ for electron showers

$C_i = +0.5$ for photon showers

Transverse dimensions are measured in terms of the Moliere radius $R_M = \frac{21.2\ MeV}{E_C} X_0$

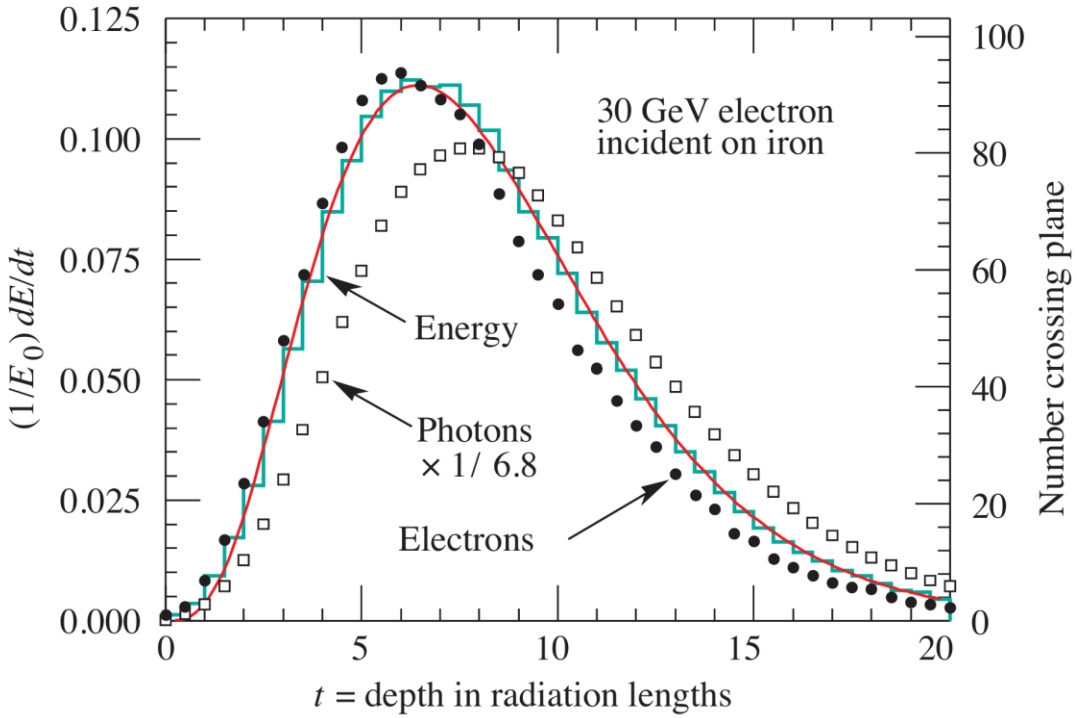

Electron, Positron Energy Loss

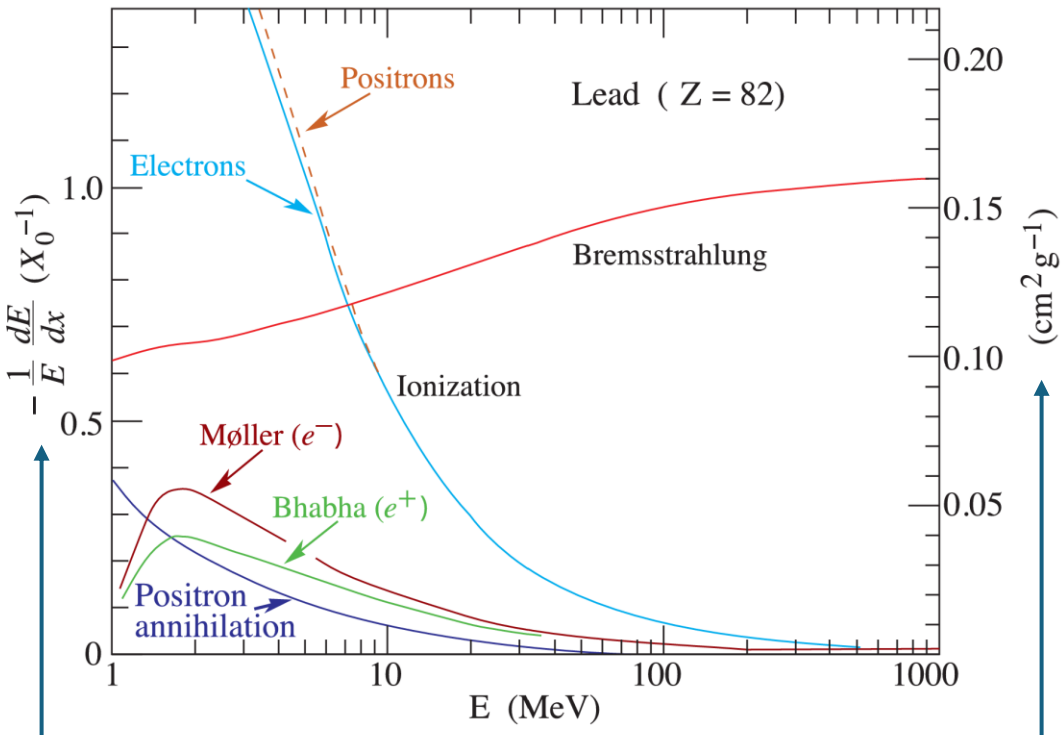

fractional energy loss per radiation length

radiation length

Photon Interactions

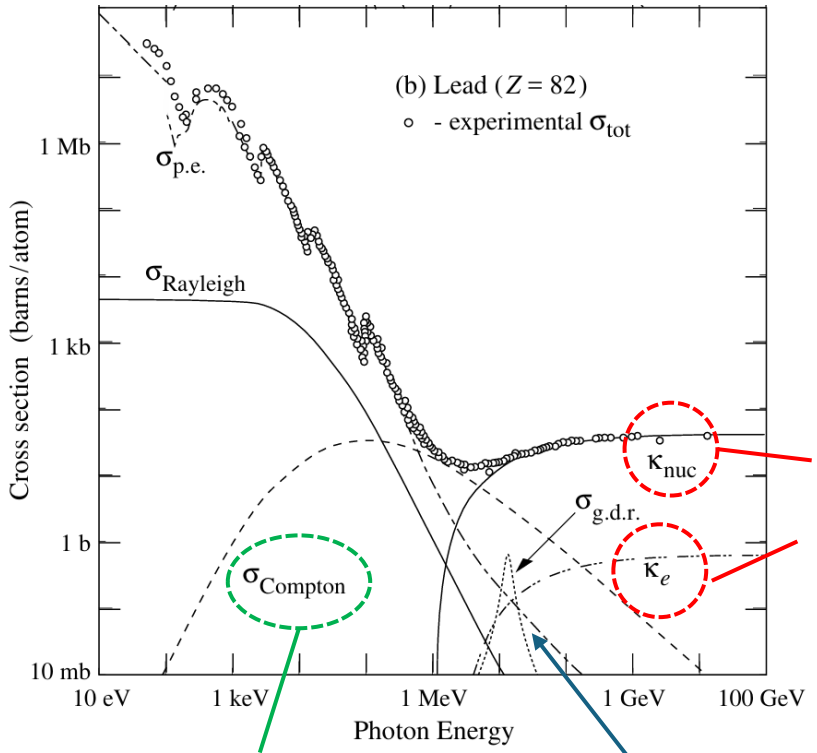

pair production

Incoherent scattering off an electron

Target nucleus broken up in photonuclear reactions (Giant Dipole Resonances)

[ASIDE] Bragg curve medical application

Real-time tracking of the Bragg peak during proton therapy via 3D protoacoustic Imaging in a clinical scenario

Siqi Wang[1,5], Gilberto Gonzalez[2,5], Leshan Sun[1], Yifei Xu[1], Prabodh Pandey[3], Yong Chen[2] ✉ & Shawn Liangzhong Xiang[1,3,4] ✉

Proton radiotherapy favored over X-ray photon therapy due to its reduced radiation exposure to surrounding healthy tissues, is highly dependent on the accurate positioning of the Bragg peak. Existing methods like PET and prompt gamma imaging to localize Bragg peak face challenges of low precision and high complexity. Here we introduce a 3D protoacoustic imaging with a 2D matrix array of 256 ultrasound transducers compatible with 256 parallel data acquisition channels provides real-time imaging capability (up to 75 frames per second with 10 averages), achieving high precision (5 mm/5% Gamma index shows accuracy better than 95.73%) at depths of tens of centimeters. We have successfully implemented this method in liver treatment with 5 pencil beam scanning and in prostate cancer treatment on a human torso phantom using a clinical proton machine. This demonstrates its capability to accurately identify the Bragg peak in practical clinical scenarios. It paves the way for adaptive radiotherapy with real-time feedback, potentially revolutionizing radiotherapy by enabling closed-loop treatment for improved patient outcomes.

S. Wang, G. Gonzalez, L. Sun, *et al., npj Imaging* **2**, 34 (2024).

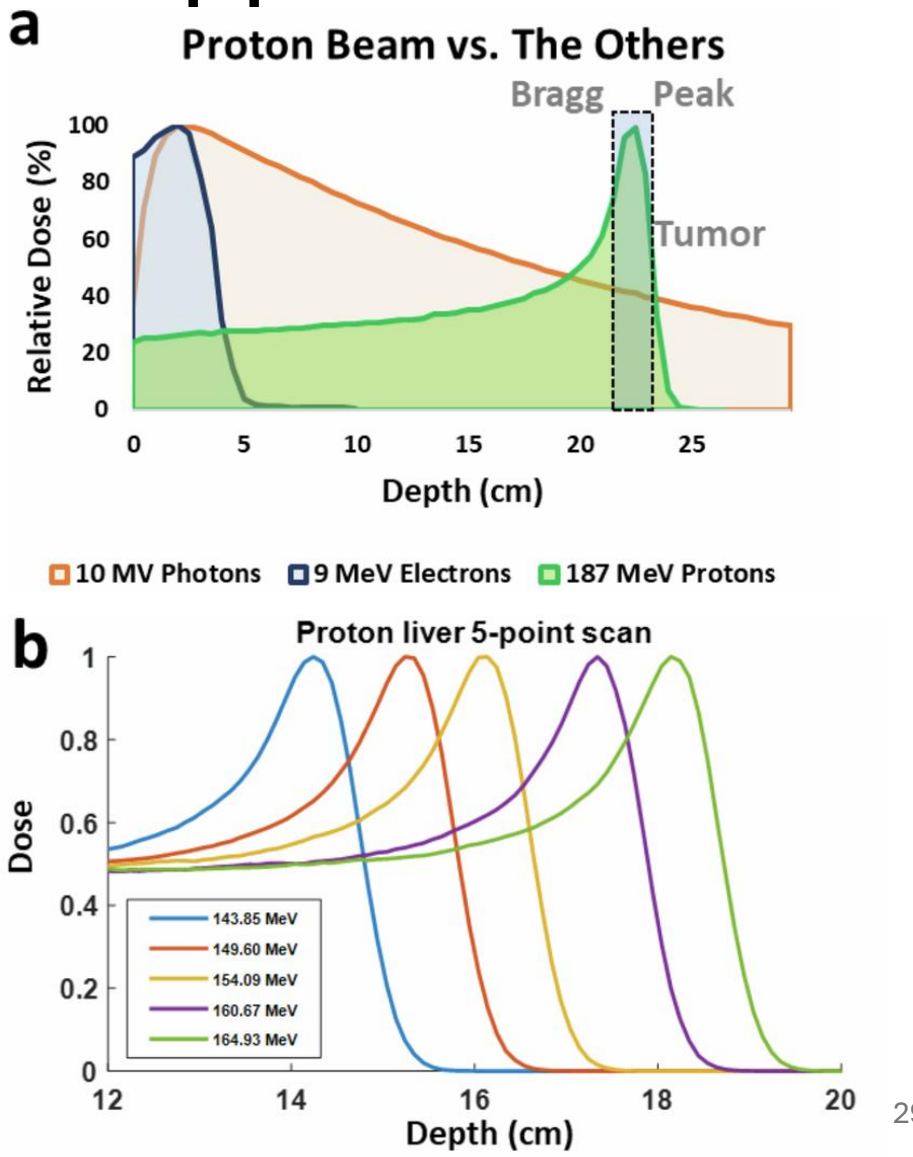

Neutron Interactions

Principally interact through the strong force

Classification by energy:

- high energy: $\geq 100\ MeV$
- “fast”: O(100) keV to O (10) MeV
- Epithermal: 0.1 eV - ~100 keV
- “slow”: energies comparable to thermal agitation energy (~1/40 eV at room temperature)

A. Friedland, S.Li, *Phys. Rev. D* **99** (2019) 3, 036009

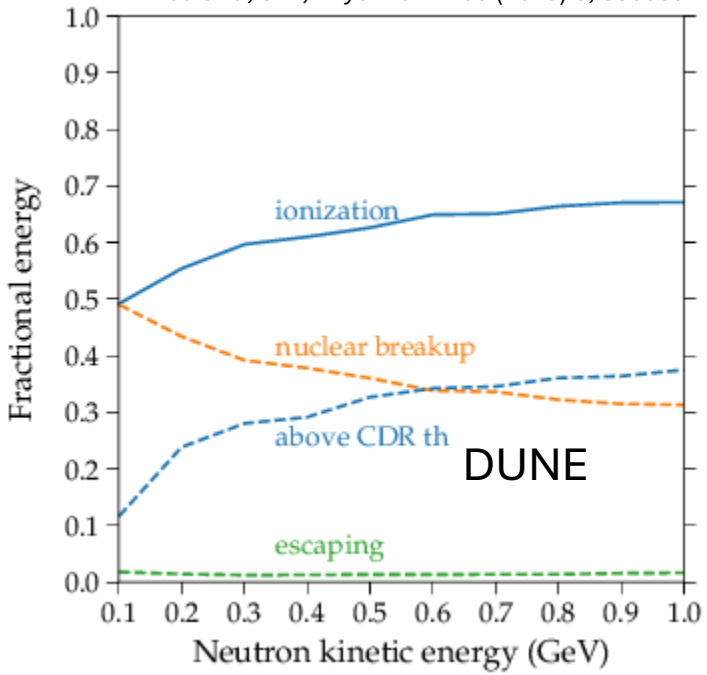

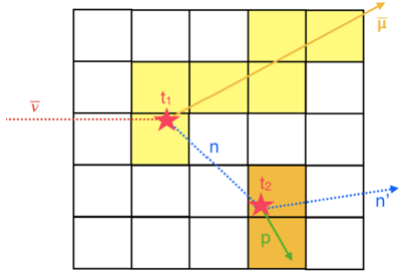

A. Agarwal *et al., Phys. Lett. B* **840** (2023) 137843

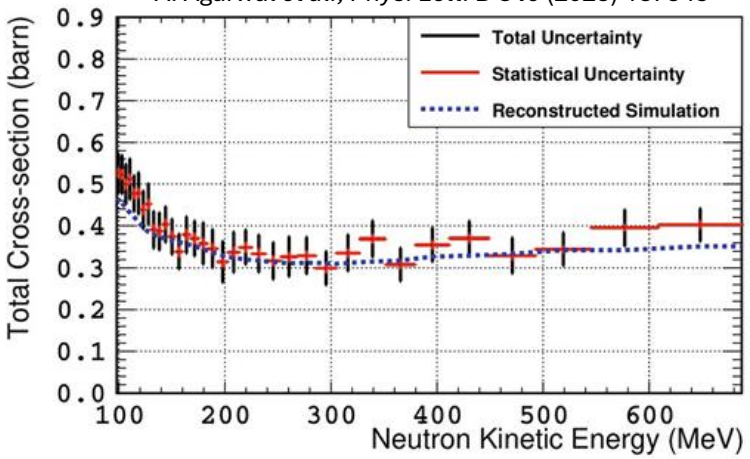

Select interaction processes:
Inelastic scattering: $A(n, n')A^*$
Radiative neutron capture: $n + (Z, A) \rightarrow \gamma + (Z, A + 1)$
Neutron capture with charged particle emission: $(n, p), (n, d), (n, \alpha), \ldots$

Outline

I. Neutrino detection
II. Signal creation
III. Principles of instrument detection & measurement

CMS DETECTOR

Total weight	: 14,000 tonnes
Overall diameter	: 15.0 m
Overall length	: 28.7 m
Magnetic field	: 3.8 T

STEEL RETURN YOKE
12,500 tonnes

SILICON TRACKERS
Pixel (100x150 μm) ~1m² ~66M channels
Microstrips (80x180 μm) ~200m² ~9.6M channels

SUPERCONDUCTING SOLENOID
Niobium titanium coil carrying ~18,000A

MUON CHAMBERS
Barrel: 250 Drift Tube, 480 Resistive Plate Chambers
Endcaps: 540 Cathode Strip, 576 Resistive Plate Chambers

PRESHOWER
Silicon strips ~16m² ~137,000 channels

FORWARD CALORIMETER
Steel + Quartz fibres ~2,000 Channels

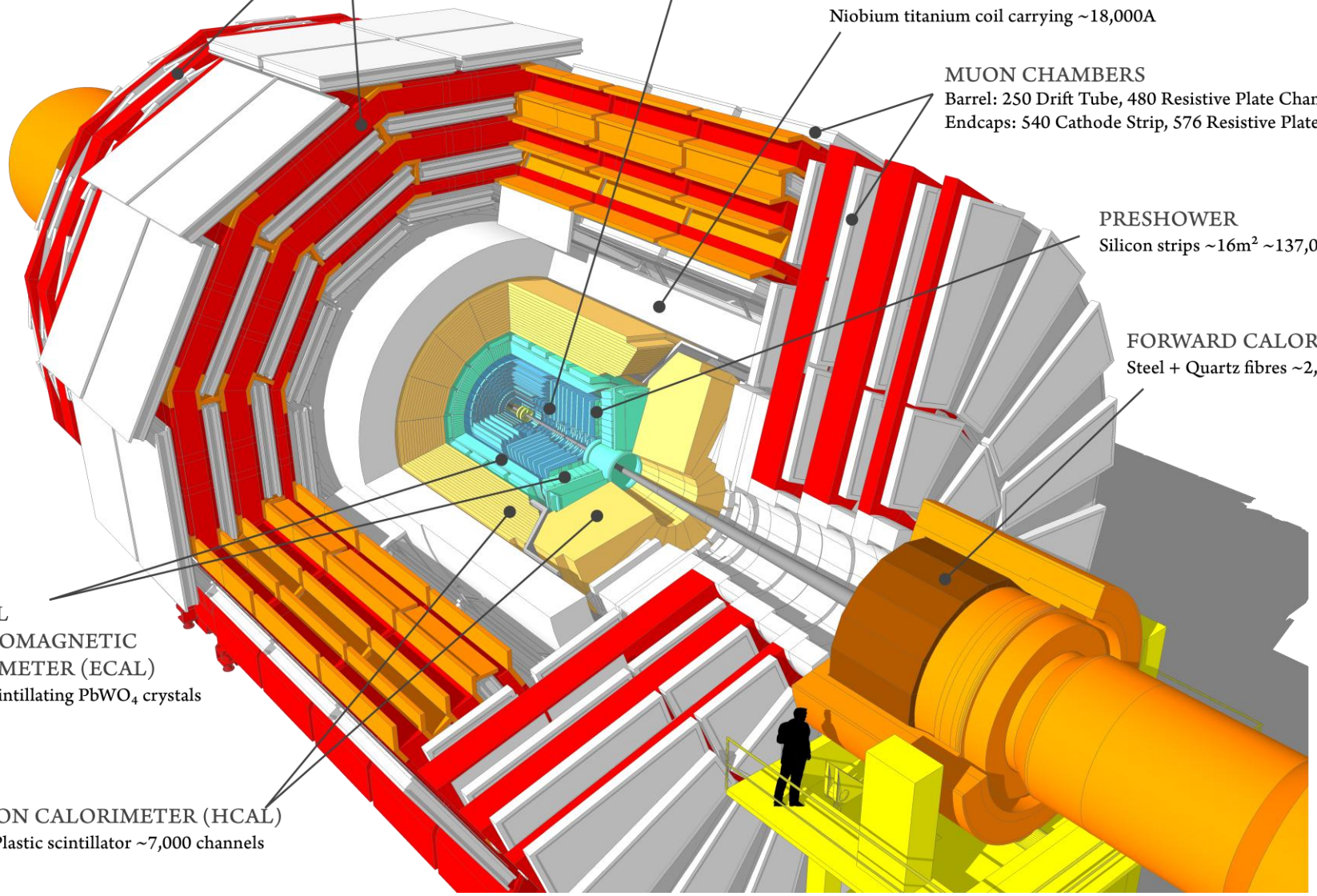

CRYSTAL ELECTROMAGNETIC CALORIMETER (ECAL)
~76,000 scintillating $PbWO_4$ crystals

HADRON CALORIMETER (HCAL)
Brass + Plastic scintillator ~7,000 channels

MINERvA Detector

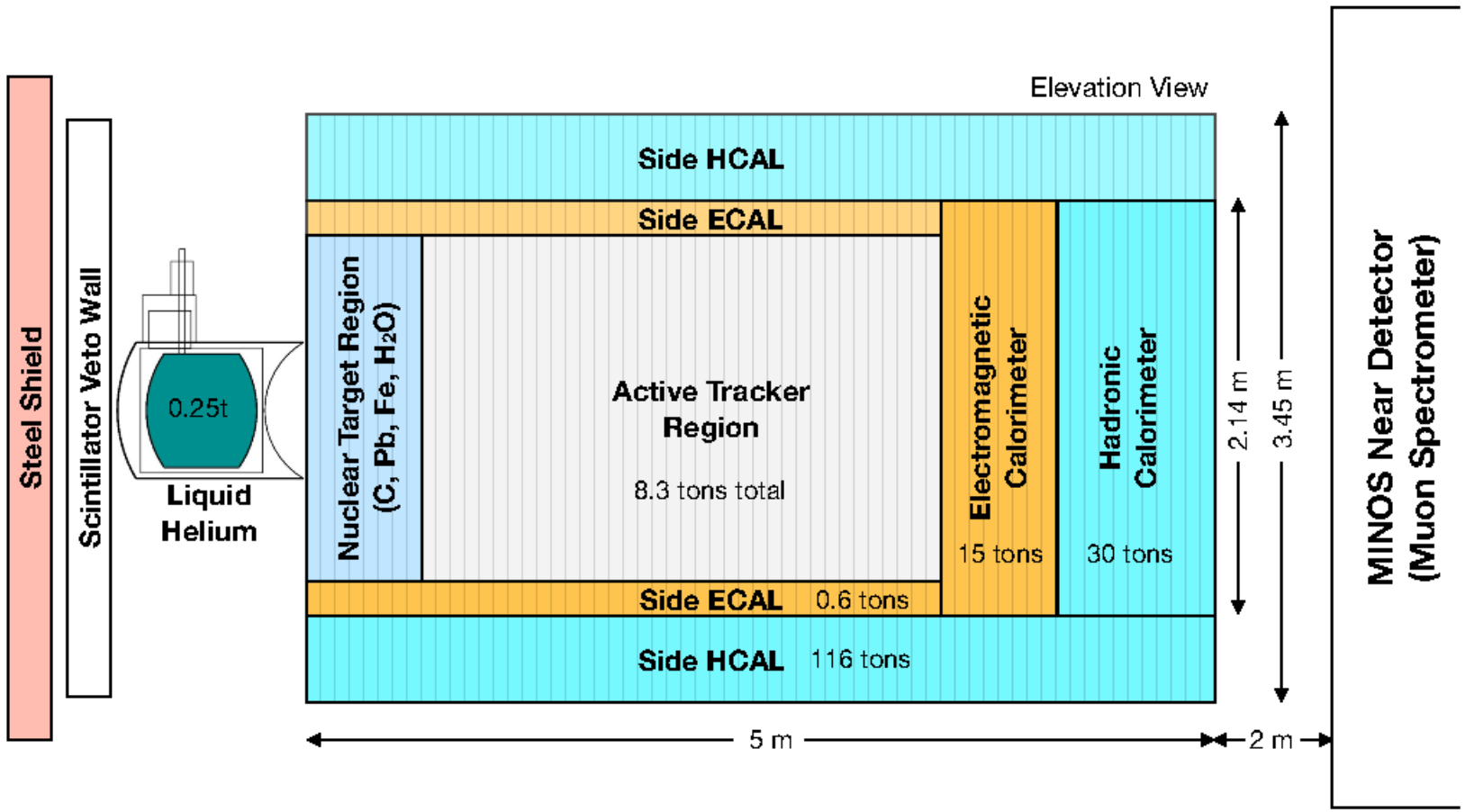

NuMI neutrino beam O(1) GeV

Key Aspects of Detector Design

Technical requirements

- Solid angle coverage
- Operation in a magnetic field
- Rate characteristics
- Position and angular resolution
- Particle identification capability
- Resolving time
- Energy resolution

Physics analysis needs

- Acceptance
- Efficiency
- Statistics
- Systematics

ν_e charged current interaction signal

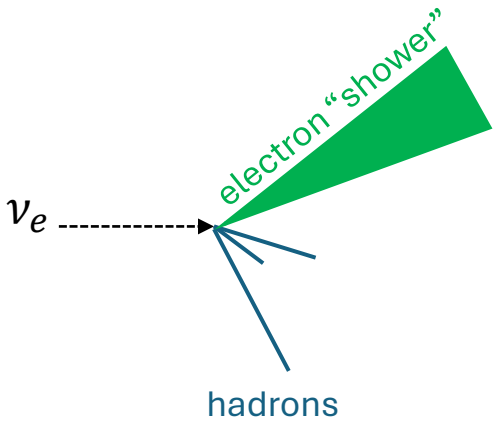

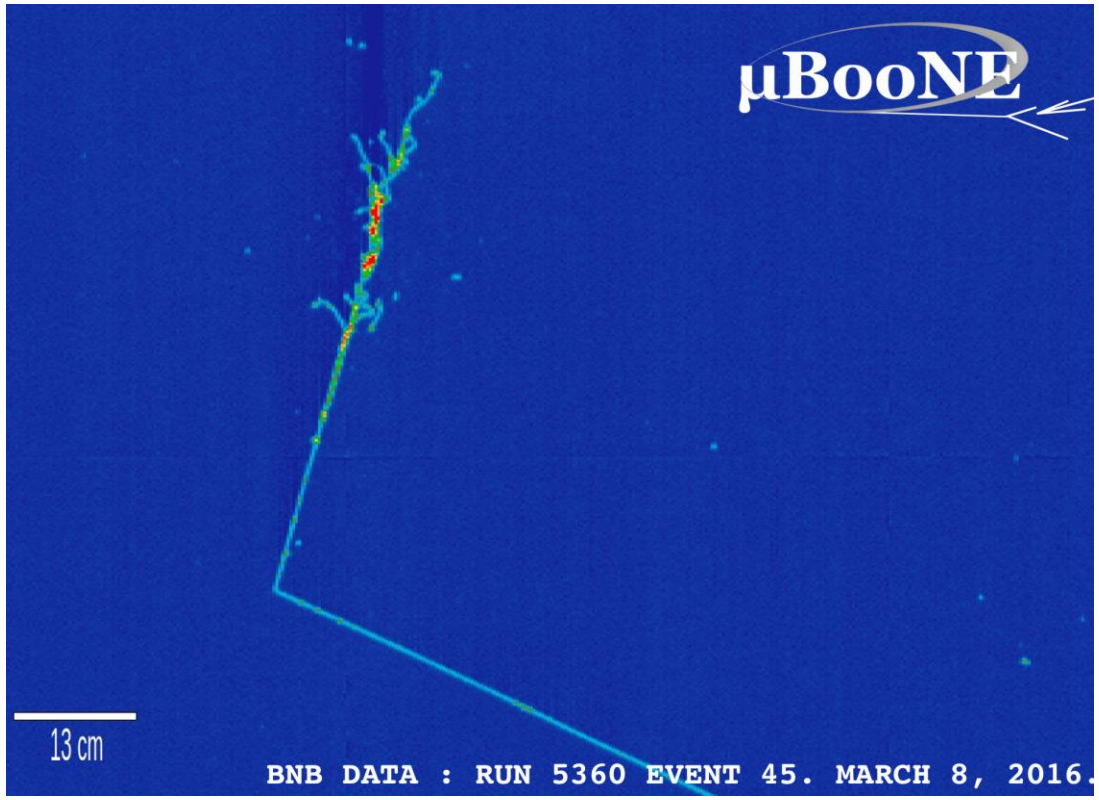

ν_e charged current interaction background

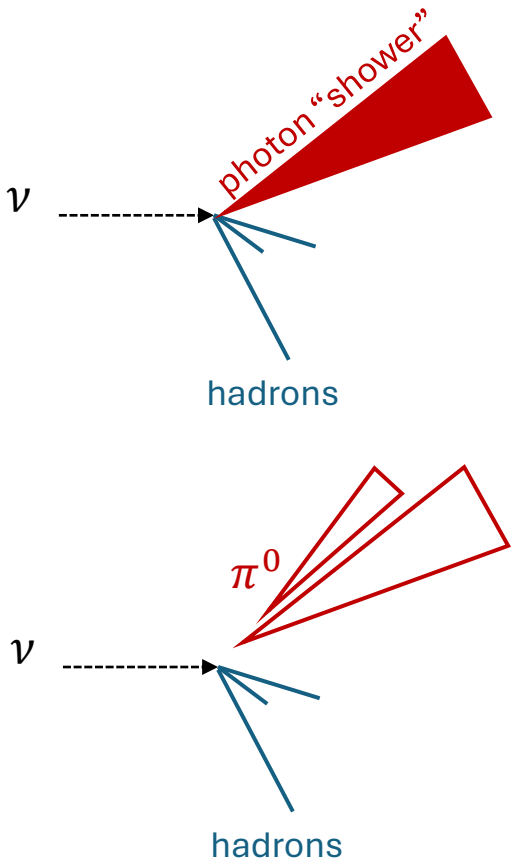

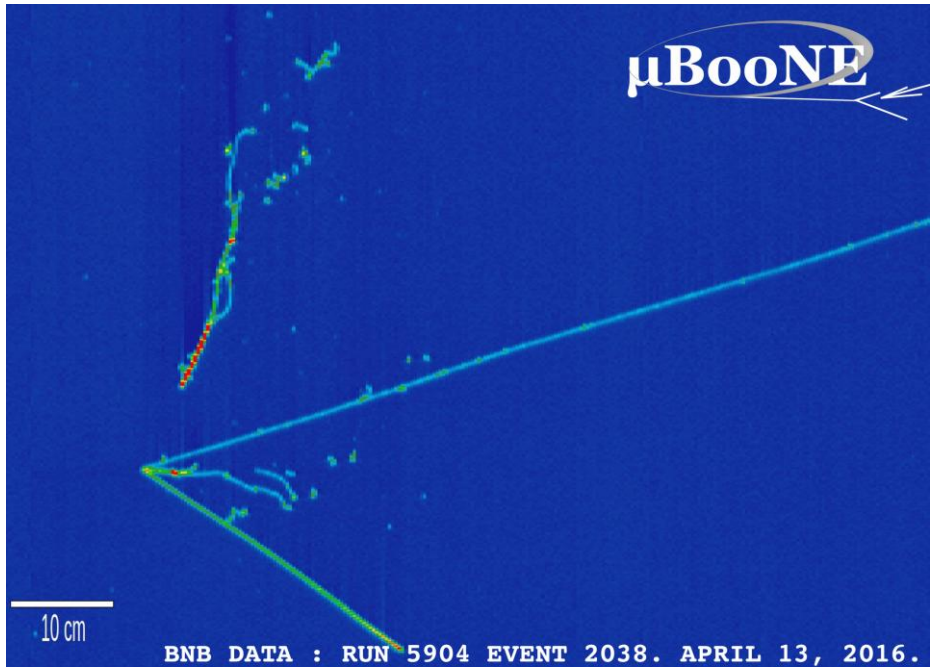

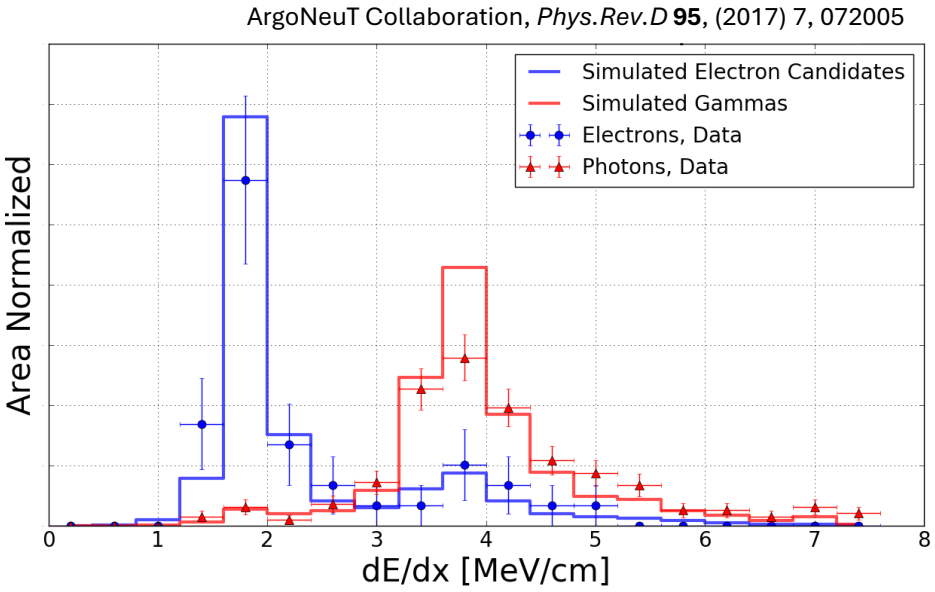

ν_μ charged current interaction signal

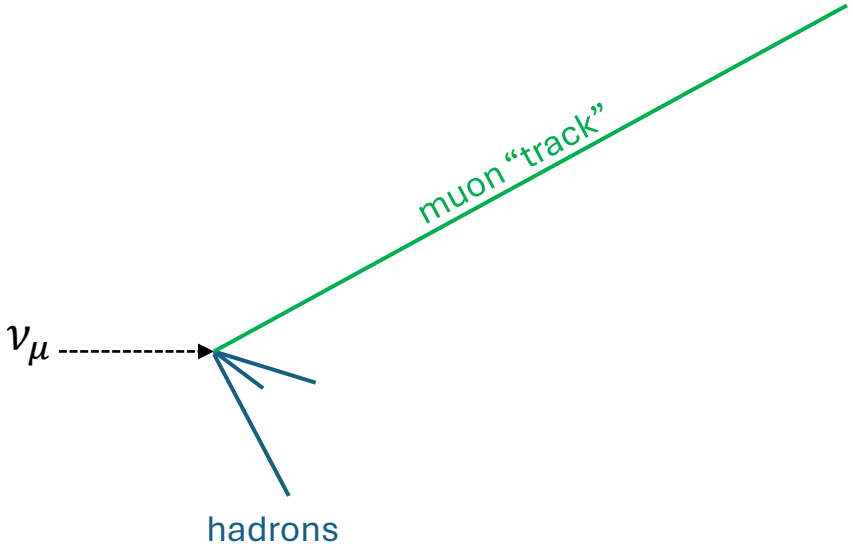

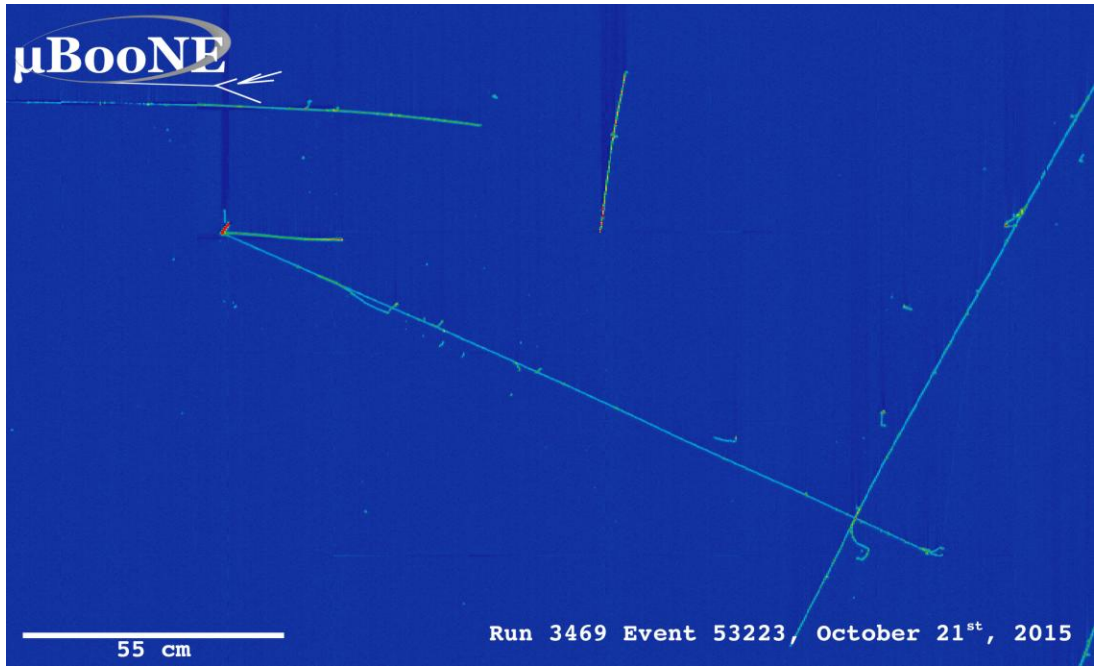

ν_μ charged current interaction background

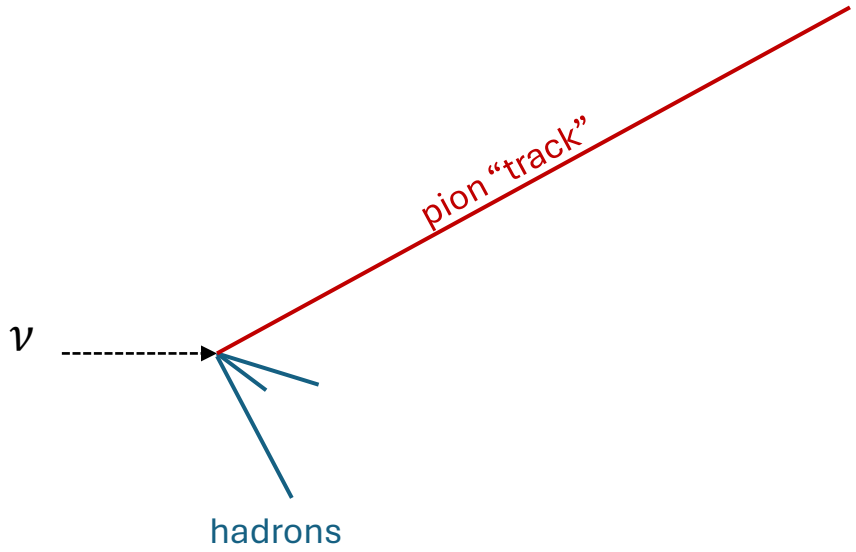

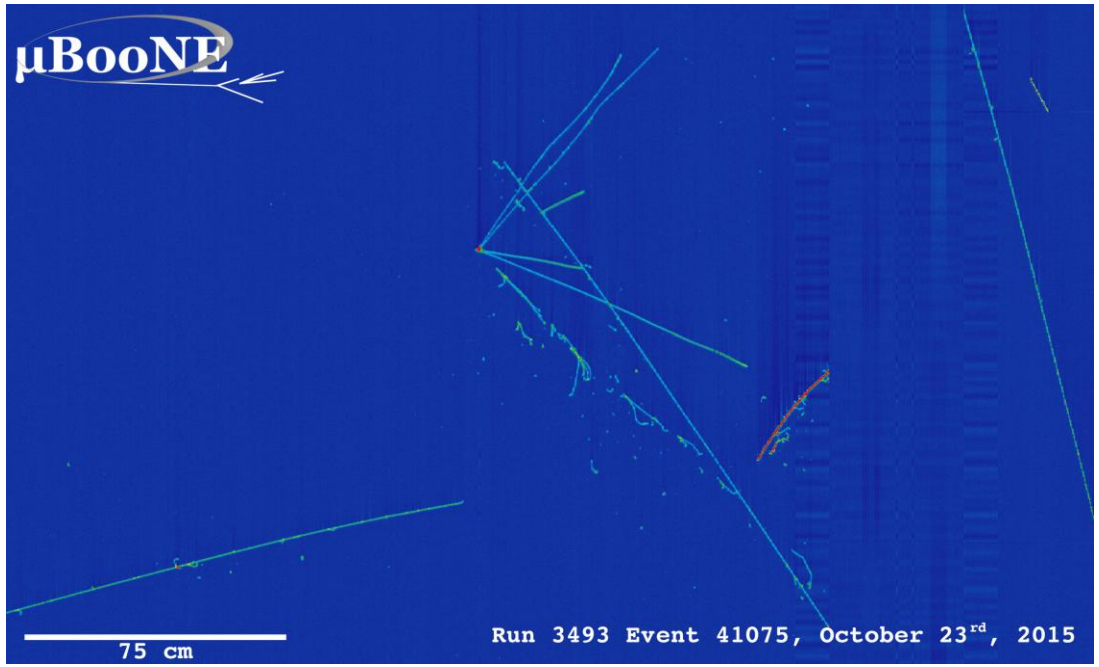

ν_τ charged current interaction signal

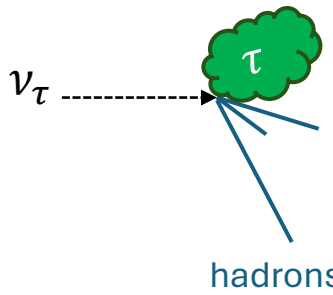

Deduced from τ decay products

Tau lepton is short lived!

$c\tau = 87.11\ \mu m$

Decay mode	Branching ratio (%)
Leptonic decays	35.21
$e^-\nu_\tau\bar{\nu}_e$	17.85
$\mu^-\nu_\tau\bar{\nu}_\mu$	17.36
Hadronic decays	64.79
$\pi^-\pi^0\nu_\tau$	25.50
$\pi^-\nu_\tau$	10.90
$\pi^+\pi^-\pi^-\nu_\tau$	9.32
$\pi^-\pi^0\pi^0\nu_\tau$	9.17
$\pi^+\pi^-\pi^-\pi^0\nu_\tau$	4.50
$\pi^-\pi^0\pi^0\pi^0\nu_\tau$	1.04
$K^-\nu_\tau$	0.70
$\pi^+\pi^-\pi^-\pi^0\pi^0$	0.55
Other	3.11

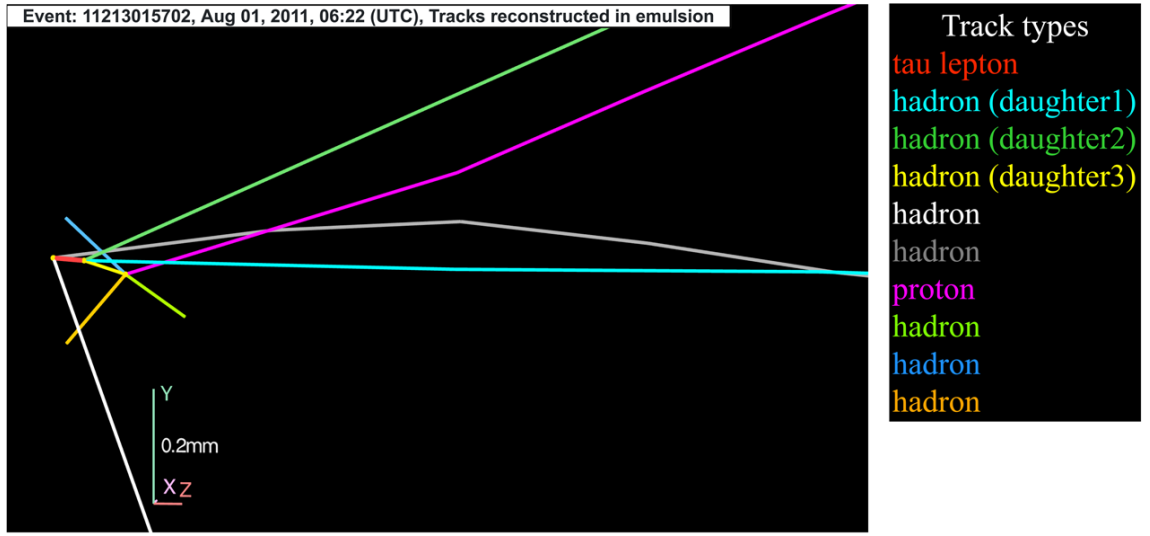

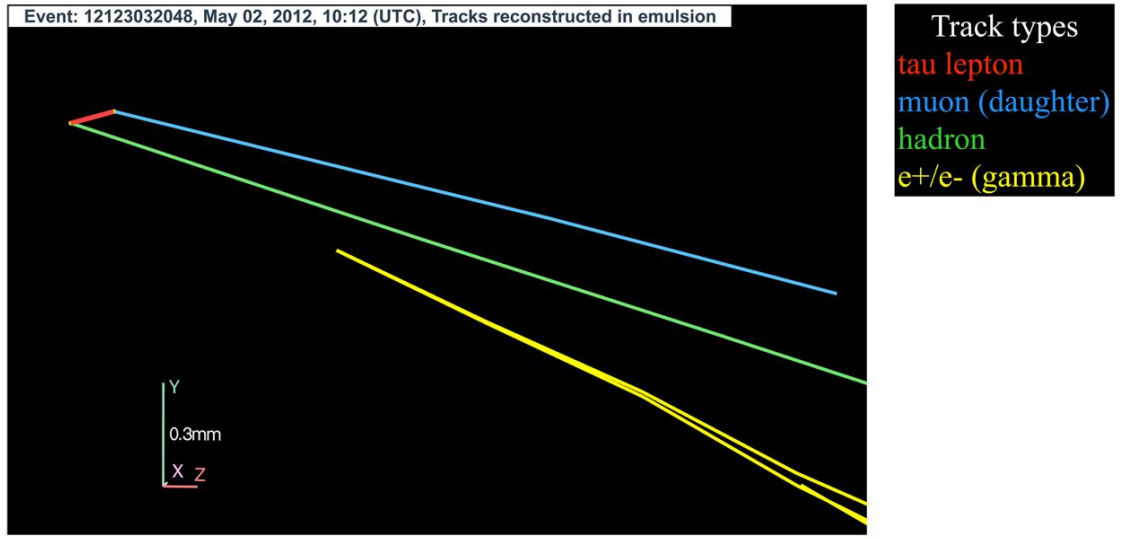

Opera Collaboration, *Sci Data* **8**, 218 (2021)

OPERA Detector

625 tons of emulsion cloud chamber (ECC) lead bricks

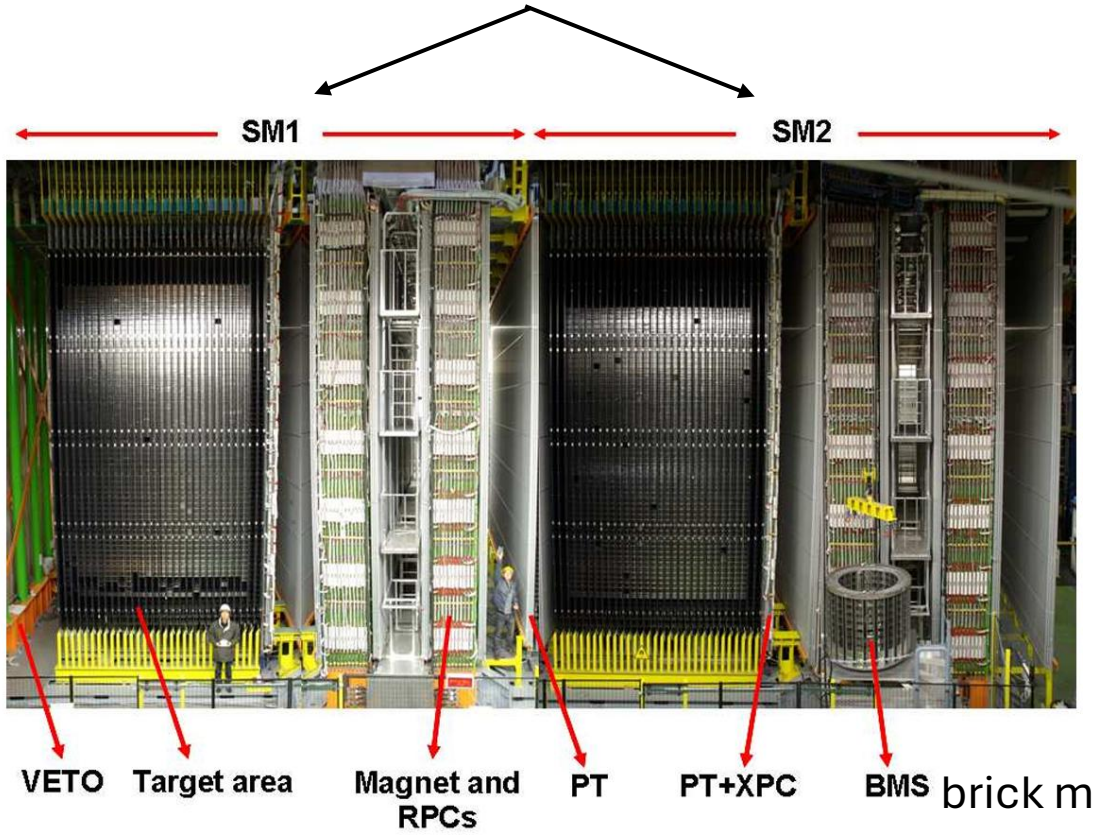

brick manipulator system

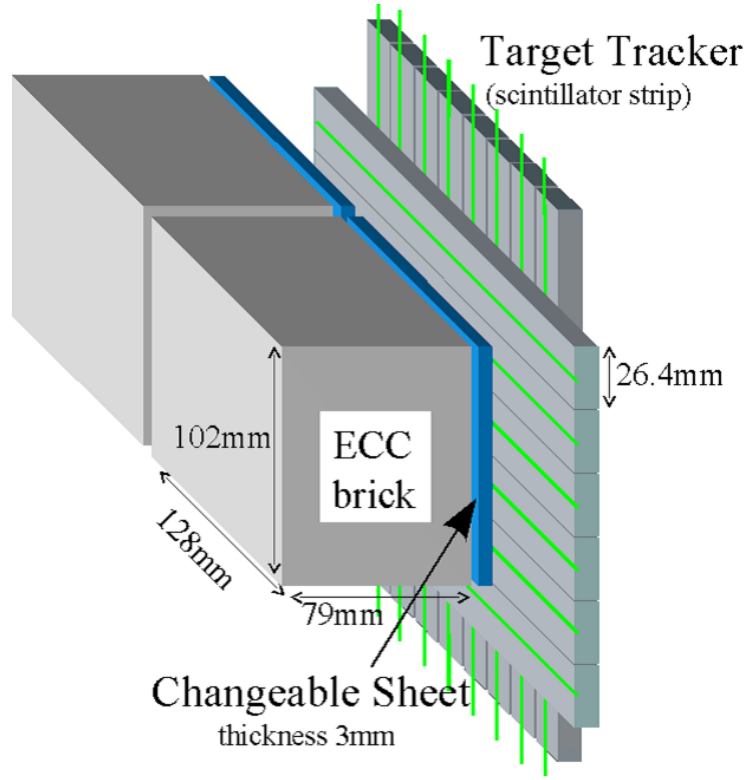

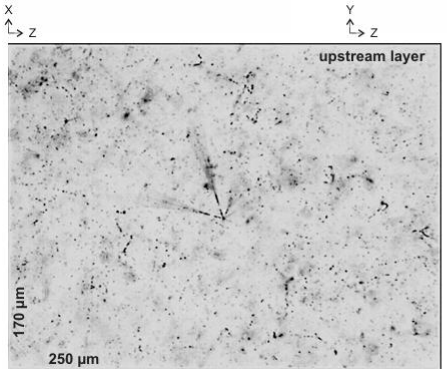

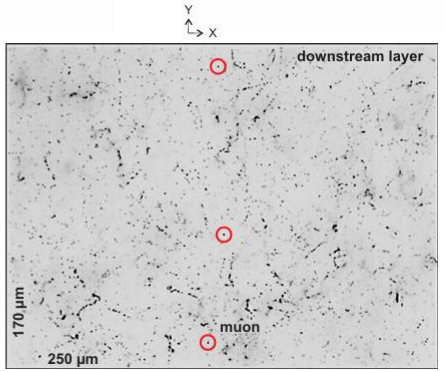

By the end of this talk, you should understand the following:

✓ How to “flavor tag” neutrino interactions

✓ Why charged leptons have specific detection characteristics

✓ How neutral current interactions can fake charged current interactions

✓ How to account for final state neutrons, to some degree